Supporting Information

Targeting Gαi/s Proteins with Peptidyl Nucleotide Exchange Modulators

Britta Nubbemeyer,[a] Ajay Abisheck Paul George,[ab] Toni Kühl,[a] Anna Pepanian,[a] Maximilian Steve Beck,[a] Rahma Maghraby,[a] Maryam Shetab Boushehri,[c] Maximilian Muehlhaupt,[d] Eva Marie Pfeil,[e] Suvi Katariina Annala,[e] Hermann Ammer,[d] Diana Imhof,[a*]and Dehua Pei[f*]

[a]Pharmaceutical Biochemistry and Bioanalytics, Pharmaceutical Institute, University of Bonn, An der Immenburg 4, 53121, Bonn, Germany. E-mail: dimhof@uni-bonn.de

[b]BioSolveIT GmbH, An der Ziegelei 79, 53757, Sankt Augustin, Germany.

[c]Pharmaceutical Technology and Biopharmacy, University of Bonn, Gerhard-Domagk-Str. 3, 53121, Bonn, Germany.

[d]Institute of Pharmacology, Toxicology and Pharmacy, Veterinary Faculty, Ludwig Maximilian University of Munich, Königinstr. 16, 80539, Munich, Germany.

[e]Molecular, Cellular and Pharmacobiology Section, Institute of Pharmaceutical Biology, University of Bonn, Nussallee 6, 53115, Bonn, Germany.

[f]Department of Chemistry and Biochemistry, The Ohio State University, 578 Biosciences Building, 484 W 12th Avenue, Columbus, OH 43210, USA, E-mail: pei@chemistry.ohio-state.edu

Table of Contents

1. Establishment of a consensus sequence

From a library of $8.6 \cdot 10^5$ peptides, ~600 positive beads were collected by their turquoise color under a dissecting microscope. 101 hit sequences (Fig. S1, Table S1) were unambiguously identified by partial Edman degradation (PED)-MALDI-TOF-MS analysis and considered for further in-depth analysis.[1,2] The examination of the hit sequences revealed, that basic ([+]: H, K, R) and large aromatic/hydrophobic amino acids (Ω: F, W, Y) occur more frequently at both N- and the C-terminal positions, whereas almost no acidic amino acids ([-]: D, E) were found (Fig. S1, Symbols according to Aasland et al.[3]). This is consistent with the previous observation that naturally occurring basic, hydrophobic peptides, such as melittin and mastoparan, act as Gα binders with a potential to influence the G protein activity.[4,5]

In the N-terminal positions P-4 to P-1, the basic amino acids Arg and Lys were more common, as were aromatic amino acids, i.e. Trp and Phe, at positions P-4 and P-3. This is in agreement with the established consensus sequence in Fig. S1c-d. In addition to the general trend of basic and hydrophobic amino acids, polar-neutral amino acids were also found in these positions as can be exemplified with Asn and Gln in P-4 as well as Ser, Thr and Tyr in P-1.

In the C-terminal positions, the basic amino acids, especially Arg, occurred in all positions most frequently. Additionally, the aromatic amino acids Tyr and Phe were commonly found in P+1 to P+4. Aliphatic amino acids (Ψ: V, I, L, Nle) occurred in many cases in P+4, while hydrophobic amino acids (Φ: F, I, L, Nle, V, W, Y,) were often detected in P+1. In P+2 and P+3, it was more common that uncharged polar amino acids (ζ: N, Q, S, T) occurred, in particular Tyr and Ser in P+2 and Gln and Asn in P+3.[3]

Overall, 13 representative peptides (**1-13**, Fig. 1) were selected for resynthesis and binding studies to verify the consensus sequence (Fig. 2c, S1, Tables S2, S3). Among the selected peptides, at least 6 out of 9 positions of the consensus sequence were covered by peptides **1** (**GPM-1**), **3**, **8** and **9**, whereas peptides **10** and **11** only matched the consensus sequence at 2 positions. However, the latter peptides were selected to cover a broad spectrum of the screening results.

2. Computational studies to visualize peptide-Gαi1/s interactions

A homology model (Fig. S10, Tables S5, S6) of Gαi1 was produced using an existing X-ray crystallographic structure (PDB: 3UMS[6]) and a first model of the NMR ensemble (PDB: 5JS8[7]) as templates in the YASARA molecular modeling suite (see Methods for details). The quality of the 3D model of Gαi thus produced was deemed optimal with a YASARA Z-score of 0.67, a Ramachandran Z-score of -0.65 and a DOPE score[8] (a non-local normalized energy Z-score of -0.61 computed by the ANOLEA webserver[9] (Table S5)). The model was subjected to a 500 ps refinement simulation[10] using the YAMBER force field. The resulting lowest energy structure was used in all further analyses (Table S6). Similarly, 3D models of the peptides (**GPM-1**, **GPM-1b-d**, **GPM-1 Y5A**, and peptide **15**) were also computationally generated (Fig. S15, Table S7) in YASARA (see Methods for details), each of which was further subjected to a 100 ns, explicit, all-atom MD simulation using the AMBER14 force field[11]. Structural equilibration of the peptides was ascertained using the computed backbone RMSD (Tables S8-S10). The final structure from the equilibrated MD trajectory of each peptide was docked on the Gαi structure via an "ensemble docking" approach[12,13] implemented in YASARA using the VINA algorithm[13]. In addition, **GPM-1**, **GPM-1 Y5A**, **GPM-1c** and **GPM-1d** were docked similarly to a Gαs crystal structure (PDB: 6EG8[14], chain I). Prior to molecular docking simulations, an exercise to predict the possible binding sites of the peptides on Gαi and Gαs was conducted using the DoGSiteScorer algorithm[15,16] embedded in the molecular modeling suite SeeSAR (Fig. S12, S13, see Methods for details). Given the homology model of Gαi with the GDP molecule removed as input, SeeSAR successfully predicted the GDP binding site on Gαi as the primary binding site comprising of 35 residues and a second 21-residue binding site between the α2 and α3 helices on the model (Fig. S12). This predicted second binding site turned out to be the site Switch II/α3 helix, where KB-752 and GIV also bound on Gαi (Fig. S11), as well as the best binding for the peptides in this study as determined by independently conducted blind docking simulations (Fig. 4, S16). Additionally, a third smaller (15 residues) binding site was predicted by SeeSAR (Fig. S11). Interestingly, the C-terminal residues of **GPM-1c** (the best binding peptide) lodged into the grooves of this site, indicating that this prediction was not a trivial one. For Gαs, the experimentally determined GDP binding site on Gαs was correctly predicted, shown as binding site 1 (29 residues) in Fig. S13. The second predicted binding site (27 residues) largely overlaps with residues of binding site 1 and turned out to be the best binding site for the peptides used in this study. This indicates that

peptide binding to binding site 2 will have a consequent effect on binding site 1 that houses the GDP molecule. A third binding site (17 residues) was also predicted to which only the peptide **GPM-1 Y5A** bound. As mentioned in the main text, since the experimental analysis could clearly classify the peptides into active (**GPM-1c** and **GPM-1d**), slightly active (**GPM-1**), and inactive (**GPM-1b**, **GPM-1 Y5A** and **15**), the extensive molecular docking and MD simulation of the docked complexes to determine relative binding energies were restricted to only these 6 peptides for Gαi and to **GPM-1**, **GPM-1c**, **GPM-1d** and **GPM-1 Y5A** for Gαs. The results of the docking exercise yielded in peptide-Gαi/s complexes sorted by VINA-predicted binding affinities (Tables S8, S9, VINA's scoring function). The top two VINA-predicted peptide-Gαi/s complexes for each peptide were further validated by the more rigorous binding affinity prediction protocol implemented by the PRODIGY server[17], where it was confirmed that best binding energies predicted by VINA also had the best PRODIGY binding energy scores (Tables S8, S9). The complex with the best predicted binding for each peptide was further subjected to a 50 ns, explicit-solvent, all-atom MD simulation. This step was undertaken in order to reproduce a physiological environment since complexes predicted via docking do not take solvent effects and the associated enthalpies and entropies into consideration. The peptide-Gαi complexes are shown in Fig. 4 and Fig. S16, the peptide-Gαs complexes are visualized in Fig. S17.

The binding of **GPM-1c** to Gαs involved multiple H-bonded contacts stabilizing the bound conformation (Fig. S17b). It was observed that this stability was further enhanced by the fact that all residues with ring moieties (Phe1, Nal2, Trp9, Tyr12 and Tyr15) strongly blanketed the protein surface with hydrophobic interactions (Fig. S17a). The largest number of H-bonded partners on the protein (among all peptides analyzed), and the additional stability conferred by the hydrophobic interactions forms a clear basis for the high binding affinity of **GPM-1c** found by both experiments and computational investigations (Fig. 2c-d, Table S12). In the **GPM-1d**-Gαs bound conformation, the residues Tyr5 and Tyr8 besides being stabilized by H-bonded interactions with the Gαs residues are involved in hydrophobic interactions with the protein surface which contributes to their stability and also to longer residence times of the aforementioned H-bonded interactions (Fig. S17e-f). Additional hydrophobic interactions between the rings systems of Phe11 and Nal12 stabilize the binding. The locked conformation induced by the cyclic moiety further orients Trp2 of **GPM-1d** to participate in hydrophobic interactions with the protein, further stabilizing the binding. In **GPM-1**, the residues Tyr5 and Tyr8 are involved in hydrophobic interactions with the protein surface, which in turn contribute to their orientations favorable for persistent H-bonds as shown in Fig. S17c-d. Trp2 stays buried in a deep hydrophobic groove formed between the Switch II and α3 structural elements. In the case of **GPM-1 Y5A**, the initial bound conformation is stabilized by hydrophobic interactions between the residues Trp2 and Tyr8 of the peptide and the protein. However, the peptide is unstable in this conformation and quickly dissociates into bulk solution only to be held by long range electrostatic forces (Fig. S17g). Similar to the Gαi-**GPM-1** interaction, the Tyr5 residue appears to be crucial for the Gαs interaction as well, since the mutant does not form a stable complex. A loss of binding affinity and activity of the KB-752 Phe8Ala mutant towards Gαs was also described, which is another indication of the KB-752-like mode of action of **GPM-1**.[18] As opposed to peptide-Gαi interactions, peptide-Gαs interactions had a proportional increase of GDP binding to Gαs as shown in Table S12 and Fig. S18. Our results thereby indicate that the active and slightly active peptides investigated in this study (**GPM-1c**, **GPM-1d**, and **GPM-1**) act as effective GDIs on Gαs.

3. Experimental Methods and Instrumentation

General chemicals and stock solutions. All reagents were purchased from commercial sources and were used without further purification. Standard coupling reagents, resins and amino acid derivatives used for solid phase synthesis were obtained from Orpegen Peptide Chemicals GmbH, Novabiochem and IRIS Biotech. Peptide synthesis reagents and solvents were of reagent grade, and solvents for chromatography were of analytical grade obtained from VWR International. Oxygen- or water-sensitive reactions were performed under argon atmosphere. Guanine nucleotides for membrane assays and tissue culture reagents were from Calbiochem and Thermo Fisher Scientific. All other reagents were from Sigma-Aldrich unless stated otherwise.

Binding studies

For the binding studies, Gα protein previously stored at -80 °C was rebuffered on a PD-10 column (SephadexTM G-25 M with 0.1% Kathon™ CG, GE Healthcare) and concentrated with an Amicon Ultra-30K (Merck Millipore Ltd.) filter. The final protein concentration was determined by Bradford assay as described above.[19]

The microscale thermophoresis (MST) measurements were performed with Monolith NT115 instruments from NanoTemper Technologies GmbH. For the Gα protein, different concentrations varying from 0.5 nM-40,000 nM were prepared by serial dilution in buffer (20 mM HEPES, 100 mM NaCl, 2 mM DTT, 1 mM $MgCl_2$, pH 8.0) containing 5% (v/v) DMSO and 0.05% (v/v) Tween20. The fluorescence-labeled peptides were dissolved in DMSO (5% (v/v) DMSO final) and diluted to a final concentration of 100 nM in the same buffer. Then, the peptide solution was diluted 1:1 with the Gα protein and incubated at room temperature for 30 min. In addition, a control without Gα protein was prepared. For the MST measurement, the solution was transferred into Monolith NT115 standard treated glass capillaries from NanoTemper. The thermophoresis was measured twice for each capillary at 50% LED power and 40% MST power. The baseline corrected data were normalized to the curve amplitude and analyzed with Graph Pad Prism 7.0 by using the following equation provided by NanoTemper (1).

$$(1)\ f(c) = unbound + (bound - unbound) \cdot (c + c_{target} + K_d - \sqrt{(c + c_{target} + K_d)^2 - 4 \cdot c \cdot c_{target}})/(2 \cdot c_{target})$$

For the competition experiment, 200 nM Cf-KB-752 and 200 nM Gαi·GDP were mixed in a 1:1 (v/v) ratio and incubated for 15 min at room temperature. Subsequently, **GPM-1** was added in concentrations ranging from 1.22-10,000 nM. The solution (50 nM Cf-KB-752, 50 nM Gαi·GDP, varying concentration of **GPM-1**) was transferred into the capillaries and the MST measurement was initiated immediately. As a control, a measurement without the addition of **GPM-1** was performed. The values obtained were normalized to the maximal deviation: complete complexation of Cf-KB-752 and Gαi1 minus the maximum displacement caused by the highest **GPM-1** concentration. The IC_{50} value was calculated by a one-site fit log IC_{50} model (equation (2)) using GraphPad Prism 7.0.

$$(2)\ Y = Bottom + (Top - Bottom)/(1 + 10^{(X - Log(IC_{50}))})$$

Surface plasmon resonance (SPR) measurements were conducted on a Biacore 8K device from GE Healthcare. All experiments were carried out at 25°C in SPR buffer (10 mM HEPES, 150 mM NaCl, 1 mM $MgCl_2$, 0.05% (v/v) Tween20, pH 7.4). A streptavidin-coated sensor chip (Series S, Sensor Chip SA, GE Healthcare) was conditioned with 1 M NaCl/50 mM NaOH according to the manufacturer's instructions. The biotinylated peptides (Btn-**GPM-1**, Btn-**GPM-1c**, Btn-**GPM-1d** and Btn-**15**) were immobilized on the sensor chip at a flow rate of 10 µl min^{-1} for 1 min to reach an increase of 600 response units for Btn-**GPM-1** and Btn-**15** and 1200 response units for Btn-**GPM-1c** and Btn-**GPM-1d**. A blank flow cell was used as a control for correction of nonspecific binding as described previously.[20] Solutions of Gαi1 (15-2,000 nM) or Gαs (7.8-1,000 nM) in SPR buffer were injected over the sensor chip for 2 min at 30 µl min^{-1}. Dissociation was monitored for 400 s applying SPR buffer. The chip surface was regenerated with 200 mM NaCl containing 10 mM NaOH for 15 s at 30 µl min^{-1} for three times. Data evaluation was carried out with the Biacore™ Insight Evaluation Software and GraphPad Prism 7.0 according to a 1:1 (Gαi1, n=1) or 1:2 (Gαs, n=2) steady state model (3).

(3) $Y = RU_{max} \cdot X^{(n/(K_d^n + X^n))}$

Cell-free ELISA-based assay

The functional activity of the test compounds on intact inhibitory and stimulatory signal transduction pathways was investigated in a cell-free system using membranes from Neuroblastoma×glioma (NG108-15 cells) hybrid cells (endogenous δ-opioid receptors; 0.67 pmol mg^{-1} membrane protein) stably transfected to express the human β2-adrenoceptor (1.03 pmol mg^{-1} membrane protein).[21] Cells were cultured in Dulbecco's modified Eagle's medium (DMEM) supplemented with 5% (v/v) foetal bovine serum, 100 µM hypoxanthine, 1 µM aminopterin, 16 µM thymidine, 100 units ml^{-1} penicillin, and 100 µg ml^{-1} streptomycin at 37 °C in a humidified atmosphere of 5% CO_2 in air. Subconfluent monolayers (70% density) were harvested, membranes were prepared as described[22] and stored in aliquots in NMT buffer (20 mM Tris·HCl, pH 7.4, containing 150 mM NaCl and 10 mM $MgCl_2$) at a concentration of 2 mg ml^{-1} protein at -80 °C. For screening of the G protein modulators, membranes were thawed and preincubated with the respective peptides for 30 min on ice. Therefore, the peptides were dissolved in DMSO to a final concentration of 200 µM (stem solution). Subsequently, each incubation experiment contained 300 µg of membrane protein and 50 µM peptide in a total volume of 300 µl of NMT buffer, which corresponds to 25% (v/v) of DMSO. Adenylyl cyclase reactions were started by the addition of 20 µl of preincubated membranes to an assay system (100 µl total volume) containing (final concentrations for all components are given) 40 mM Tris·HCl, pH 7.4, 0.2 mM EGTA, 0.2 mM DTT, 100 mM NaCl, 10 mM $MgCl_2$, 0.5 mM ATP, 5 µg ml^{-1} phosphocreatine, 5 IU ml^{-1} creatine phosphokinase, 10 µM GTP, 10 µM IBMX (3-isobutyl-1-methylxan-thine), 5% (v/v) DMSO and 10 µM of the peptides. The mixture was kept at 37 °C for 10 min and stopped by the addition of ice-cold 10 mM HCl (500 µl). Adenylyl cyclase activity was determined in the absence (basal) or presence of forskolin, isoproterenol and DADLE (10 µM each) in order to assess the effect of test compounds on direct or receptor-mediated stimulation and inhibition of adenylyl cyclase, respectively.[22] The amount of cAMP generated was determined by a generic cAMP ELISA after acetylation of the samples.[23] cAMP levels were normalized to forskolin-stimulated cAMP values in control experiments using the solvent DMSO alone and evaluated using GraphPad Prism 7.0.

Whole cell HTRF-based assay

HEK293 cells were obtained from the American Type Culture Collection (ATCC) and maintained in humidified atmosphere at 37 °C and 5% CO_2. The HEK293 cells were cultured in DMEM and were tested negative by PCR for mycoplasma contamination. The homogeneous time-resolved fluorescence (HTRF)-based assay was carried out according to manufacturer's instructions (Cisbio GmbH) as described previously.[24-26] In brief, 500 cells/well were suspended in assay buffer containing 1 mM IBMX and incubated in a 384-well, white microtiter plate for 15 min. To determine inhibitory effects of the compounds, cells were preincubated with ligands (dissolved in DMSO, final DMSO concentration: 0.05% (v/v)) or solvent for 2 h prior to stimulation with 100 µM Iper-6-phth[27,28] for further 30-35 min. Reactions were terminated by addition of lysis buffer containing the HTRF® reagents. All incubation steps were carried out at 37 °C and 5% CO_2. After incubation for at least 1 h at room temperature, HTRF ratios were measured using the Mithras LB 940 multimode reader (Berthold technologies) at 665 nm and 620 nm, then converted to nM values according to the manufacturer's instructions and normalized to the isoproterenol signal.[24]

MTT-assay

HEK 293 cells were purchased from Sigma-Aldrich. The cells were maintained in DMEM supplemented with 10% FBS, 50 µg ml^{-1} streptomycin and 50 U ml^{-1} penicillin, and were cultivated in a 37 °C incubator with 5% CO_2 and 95% humidified air. The toxicity of the peptides for the cells was determined using the MTT assay. Briefly, the cells were seeded in 96-well culture dishes with a density of $2.5 \cdot 10^4$ cells per well. Following adherence, the cells were incubated overnight with various concentrations of different peptides. The next day, the supernatant was removed and the cells were incubated with MTT solution (0.5 mg ml^{-1}) for 90 min. Following the aspiration of the supernatant, the MTT crystals were dissolved in MTT, and the absorbance was measured at 540 nm. Survival was expressed as percent relative to the untreated control.

4. Computational Methods

Molecular modeling of peptide structures

Owing to the lack of experimentally resolved 3D structures for the peptides (**GPM-1**, **GPM-1b-d**, **GPM-1 Y5A**, and **15**) a computational modeling approach was pursued (Fig. S15). The YASARA (version 19.7.17)[29,30] modeling suite was used as the primary tool in this effort. As the first step, peptide sequences in the FASTA format were loaded into YASARA. At this point the non-standard amino acid residues (L-2-naphthylalanine (2Nal), (S)-2,3-diaminopropionic acid (Dap) and isophthalic acid (Ipa)) in the peptides were substituted by standard amino acid residue placeholders before they were manually changed to their desired structures as follows. The 2Nal residues in **GPM-1c**, **GPM-1d**, and **15** as well as Ipa in **GPM-1d** were initially loaded as phenylalanine residues in the FASTA format before the appropriate structural changes were manually introduced. Similarly, a serine residue served as initial placeholder for Dap in **GPM-1d**. Amide C-terminal caps were added to all peptides as part of the initial structural assembly. The appropriate peptide cyclization steps were also done manually in YASARA (for **GPM-1b** and **GPM-1d**) on the linear structures. At this stage most peptides sported bonds with unnatural lengths and were therefore subject to an energy minimization. Herein a protocol combining steepest descents and simulated annealing as implemented by YASARA was used with Amber ff14SB[11] as the force field. Force field parameters for all non-natural amino acids were derived using the AutoSMILES (http://www.yasara.org/autosmiles.htm) method implemented in YASARA. The method uses the AM1-BCC[31] model to compute atomic partial charges and the General Amber Force Field (GAFF)[32] to determine the remaining force field terms. The energy-minimized peptide structures thus built were used as starting coordinates in all further computational analyses in the current study. Analysis and energy minimizations were performed using the YASARA molecular modeling software (YASARA structure, Version 20.4.24, YASARA Biosciences GmbH). The YASARA2 force field was used for energy minimization by simulated annealing, including the optimization of the hydrogen bond network and the equilibration of the water shell, until system convergence was achieved. The molecular graphics were created using YASARA (YASARA structure, Version 20.4.24, YASARA Biosciences GmbH, www.yasara.org) and POVRay (Persistence of Vision Raytracer Pty. Ltd., www.povray.org).

Homology modeling

A homology model of Gαi, used as the target structure in all molecular docking simulations in this study was produced using the protocol available in YASARA (Version 20.4.24). The target sequence along with explicitly defined template structures namely PDB: 3UMS[6], PDB: 5JS8[7] and PDB: 1Y3A[33] fed in as inputs to the program. The individual steps that were automatically performed by the program without further user intervention as described earlier.[33]

Molecular docking studies

Based on experimental consensus, blind docking simulations were conducted wherein the resultant structures from the MD simulations of the peptides (**GPM-1**, **GPM-1b-d**, **GPM-1 Y5A**, peptide **15**) were docked to the created homology model of Gαi and Gαs (PDB: 6EG8[14], chain I). Blind docking protocols are usually used to scan for possible binding sites and binding modes of peptide ligands over the surface of the target proteins. Following an "ensemble docking" protocol[12,13], the best docked poses of peptides-protein complexes based on the predicted binding energies were chosen and analyzed. "Ensemble docking" as implemented in YASARA produces an ensemble of multiple receptor conformations by generating multiple side-chain rotamers on a fixed backbone. This method has been successfully employed in previous studies involving peptide docking.[34]

Molecular dynamics simulations

Molecular dynamics (MD) simulations were carried out to accomplish two main tasks. First, 100 ns MD simulations were run to generate a 3D conformational ensemble for the peptides (**GPM-1**, **GPM-1b-d**, **GPM-1 Y5A**, peptide **15**). Next, 50 ns refine, equilibrate, and obtain binding energy estimates from the Gαi-peptide and Gαs-peptide (**GPM-1b** and peptide **15** not conducted) complexes obtained from molecular docking experiments. The simulations were conducted using the standard protocol (md_run.mcr) available in YASARA, using the Amber ff14SB[11] force field. As explained earlier, force field parameters for the non-canonical amino acids in the peptides were derived on-the-fly using the AutoSMILES method implemented in YASARA. The rest of the setup for the simulations were maintained identical to previously described protocols.[33,34] Estimation of binding energies of the Gαi-peptide and Gαs-peptide complex using the Molecular

Mechanics Poisson-Boltzmann Surface Area (MMPBSA) method as implemented in YASARA was done identical to previous instances.[34,35]

Analysis of molecular simulation data

MD trajectories produced by YASARA were converted to the PDB format and imported into VMD (version 1.9.3) for analysis of the evolution of structural and energetic properties. SeeSAR 10.1 (BioSolveIT GmbH, 2020, www.biosolveit.de/SeeSAR) was used to analyze the atomic contributions to the binding energies of selected Gαi·GDP and Gαs·GDP simulation snapshots, using the HYDE scoring function[36] implemented in the program. Furthermore, the depiction of HYDE coronas on different bound conformations of the GDP molecules from different simulation snapshots served as a fast and visual means to understand the atomic contributions to the affinity in each case. SeeSAR was also used in the independent identification and validation of the potential binding sites for the peptides on Gαi using the DoGSiteScorer algorithm[15]. Molecular graphics were generated using VMD, SeeSAR and YASARA.

Accession codes

All structures used for the computational analyses in the current articles are deposited in the PDB under the accession codes 5JS8, 3UMS, 1Y3A, and 6EG8.

5. Supporting Figures

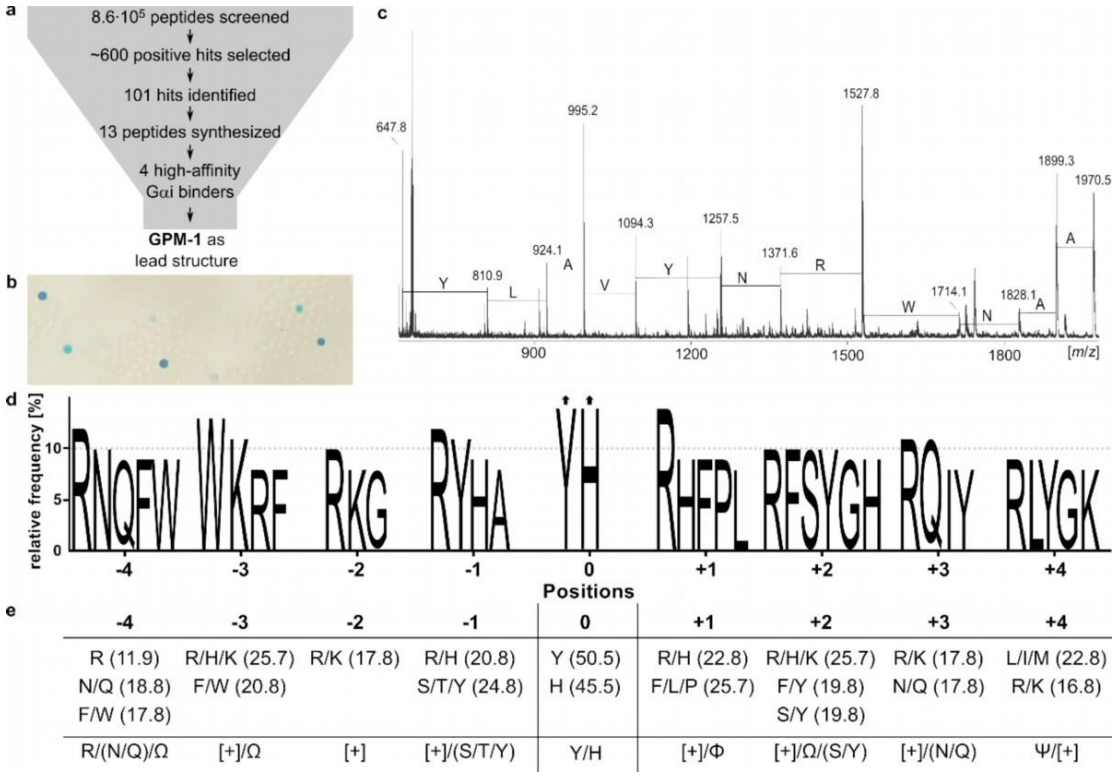

Figure S1. Development of a consensus sequence for Gαi1 binders based on the peptide library screening with Gαi1·GDP. a: Schematic representation of the hit identification and selection. **b**: Identification of Gαi1·GDP binders after incubation with 0.1 nM protein for 1 h and subsequent detection by incubation with BCIP-substrate (5-bromo-4-chloro-3-indolylphosphate) and dye precipitation.[1] **c**: Example of a representative PED-MALDI-MS spectrum of a hit sequence, i.e. NWRNYVALY. **d**: Relative frequency of amino acids (≥ 8%) at positions P-4 to P+4 relative to position 0 (Po, C/H/Y,[37]). **e**: Amino acid preferences at the different positions are given relative to Po. The postulated consensus sequence is written in the one-letter code and according to Aasland et al.[3] as follows: Φ: hydrophobic (V, I, L, F, W, Y, M), Ω: aromatic (F, W, Y), Ψ: large aliphatic (V, I, L, M), π: small (P, G, A, S), ζ: uncharged hydrophilic (N, Q, S, T), [+]: basic (H, K, R) and [-]: acidic (D, E) amino acids; M = norleucine (Nle)[37].

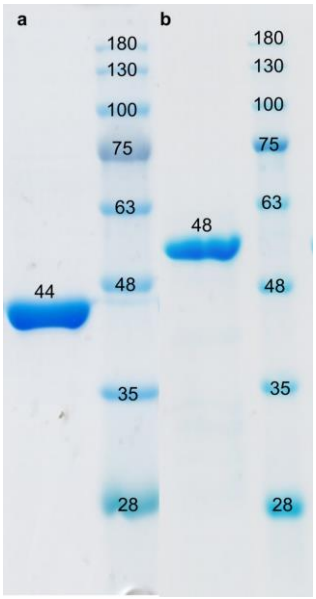

Figure S2. SDS-PAGE analysis of recombinantly expressed and purified Gαi (a) and Gαs (b) proteins. The His-tagged proteins were transformed in *E. coli* BL21 (DE3) cells.

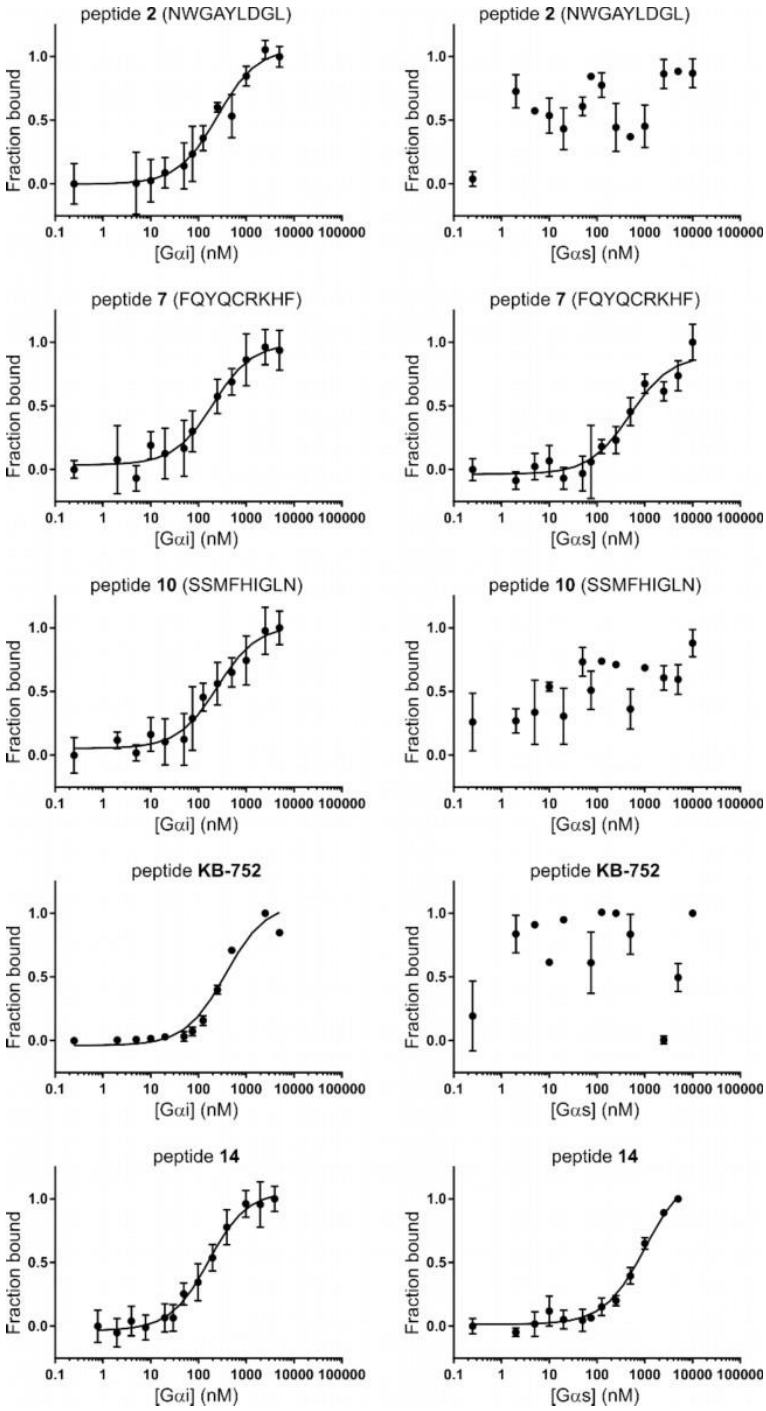

Figure S3. Binding curves obtained from the MST experiment. Binding curves of 50 nM 5(6)-carboxyfluorescein-labeled peptides **2**, **7**, **10**, **14** and KB-752 with Gαi1 and Gαs. M = norleucine (Nle)[37].

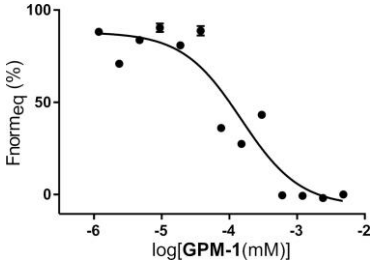

Figure S4. Competition assays of peptide 1 (GPM-1) and Cf-KB-752. After preincubation of 5(6)-carboxyfluorescein-labeled KB-752 (final 50 nM) and Gαi1 (final 50 nM) various **GPM-1** concentrations (0.61-5000 nM) were added and the changes in the thermophoretic effects were measured.

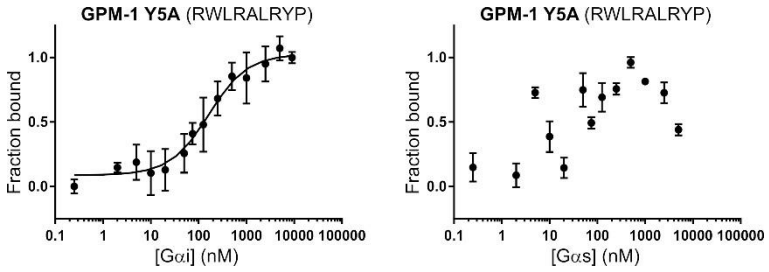

Figure S5. Binding curves obtained from the MST experiment. The binding of 50 nM 5(6)-carboxyfluorescein-labeled **GPM-1 Y5A** (also referred to as **1Y5A**) with Gαi1 and Gαs was observed using a NanoTemper Monolith NT115 device. The comparison experiment of **GPM-1** (peptide **1**) and **GPM-1 Y5A** with Gαi1·GDP showed that the K_d value of the **GPM-1 Y5A** mutant was approximately two times higher than that of **GPM-1**. In the experiment with Gαs·GDP, no binding was obtained for the **GPM-1 Y5A** mutant.

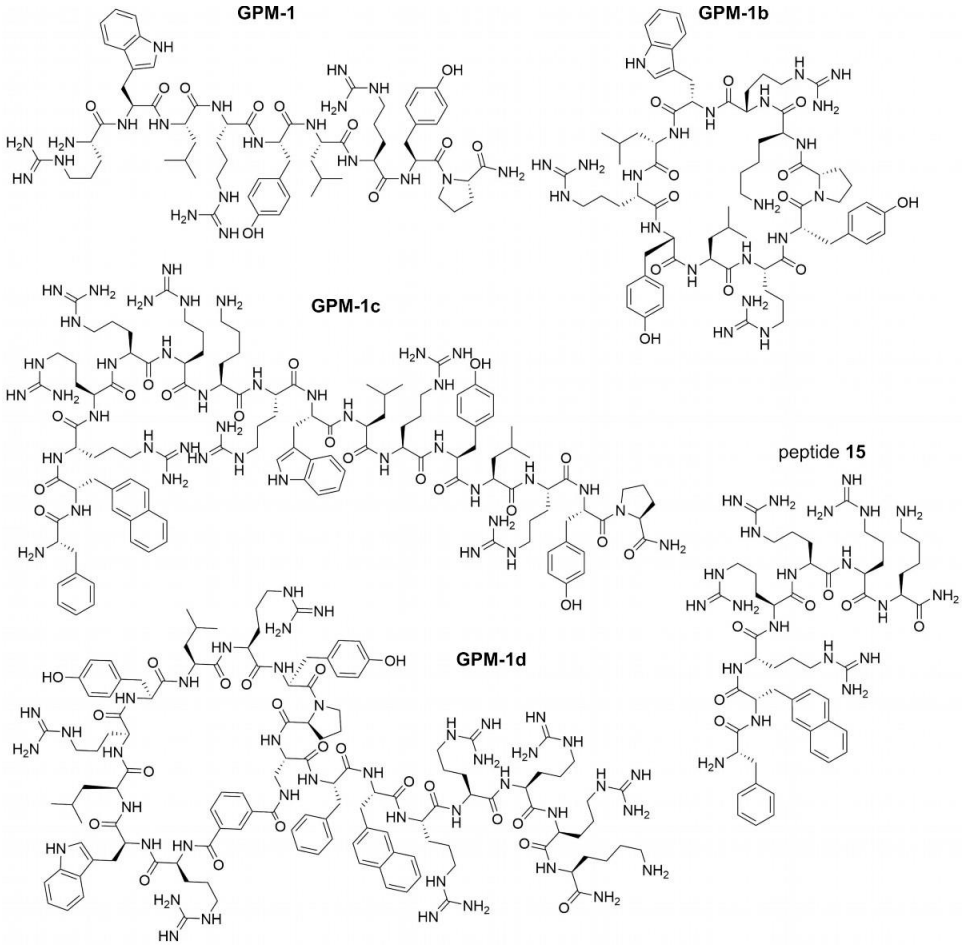

Figure S6. 2D structures of GPM-1, 15 and the GPM-1-derived peptides GPM-1b, GPM-1c and GPM-1d. The 2D structures were drawn with ChemDraw Prime 16.0.

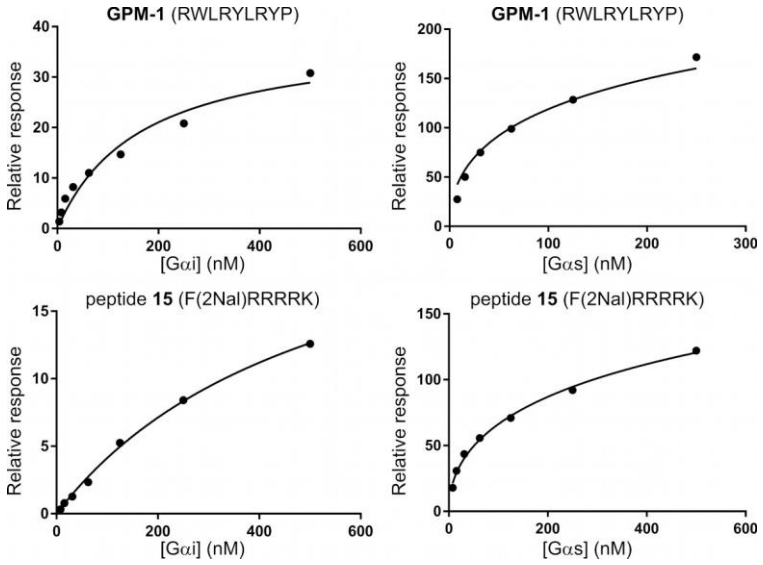

Figure S7. Binding curves obtained from the SPR experiment. Binding curves of immobilized biotinylated **GPM-1** and peptide **15** with Gαi1 and Gαs.

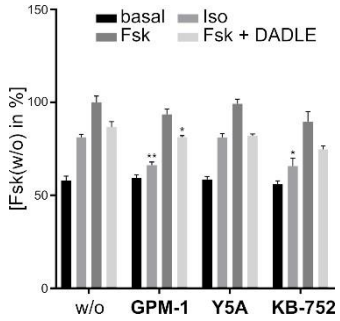

Figure S8. Relative cAMP levels on differently induced NG108-15 membrane preparations incubated with or without potential G protein modulators (**GPM-1**, **GPM-1 Y5A** and KB-752) in the presence of a phosphodiesterase inhibitor. cAMP levels were normalized to Fsk of w/o. Shown are percentage values of membranes incubated in the absence (basal), or in the presence of Iso, Fsk and Fsk+DADLE. Error bars represent SD for n=3. Statistical analysis was performed using the One-Way ANOVA Test Dunnet corrected, with *p<0.05, **p<0.01, and ***p<0.0001 for comparisons with the control (w/o).

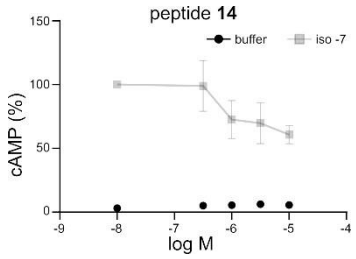

Figure S9. Iso-induced cAMP accumulation in HEK293 cells. Depicted are the buffer controls (black) and the Iso values (grey) for peptide **14** in % cAMP. Error bars represent SD for n=3.

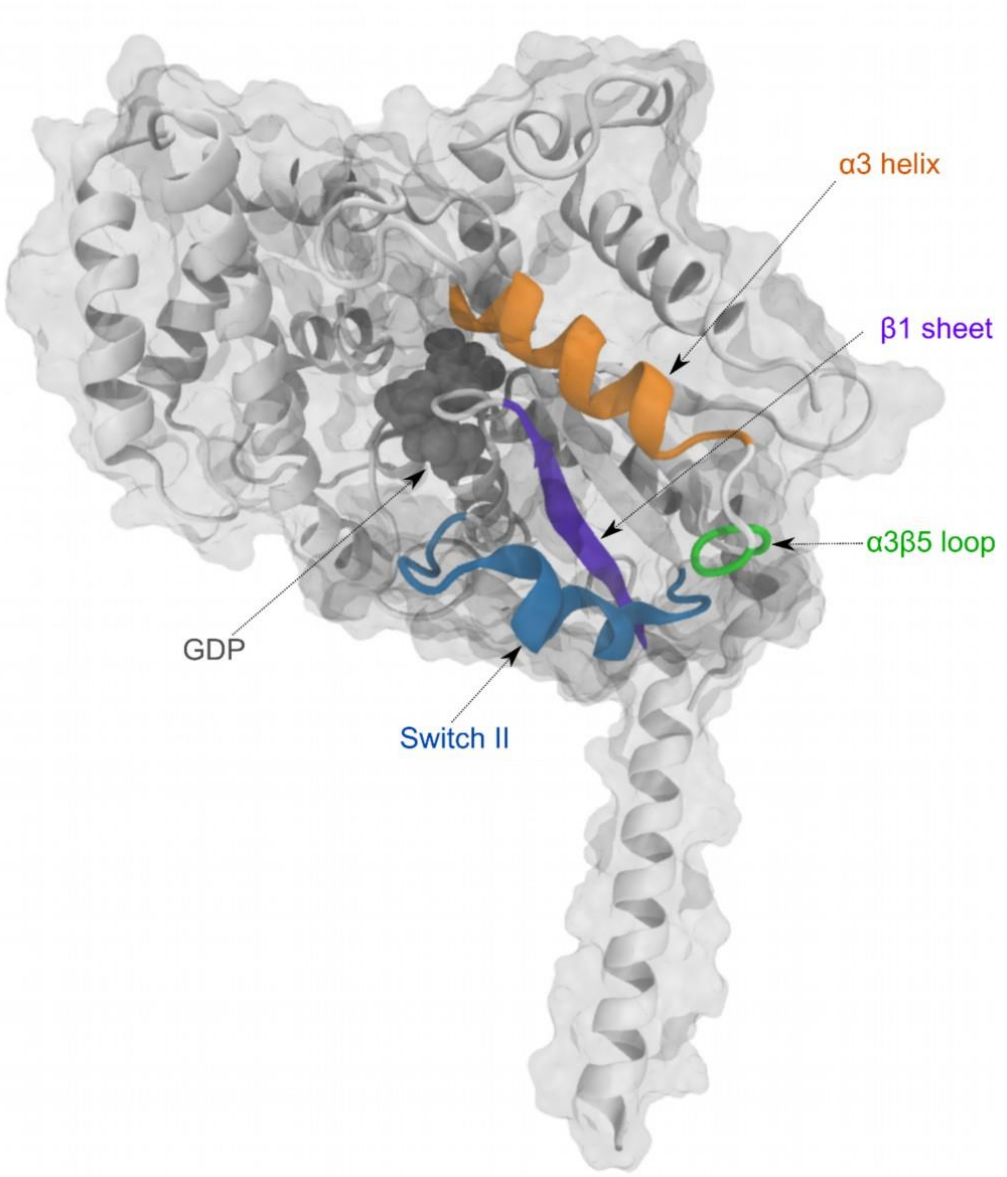

Figure S10. Homology modelling of Gαi. Homology modeled structure of Gαi created in this study, used as receptor structure in subsequent docking, and molecular dynamics simulations. The structure is depicted as white ribbons with its molecular surface representation overlaid. The segments Switch II (blue), α3 (orange), β1 (cyan), and the α3-β5 loop (green) that house the known inhibitor KB-752 are distinctly highlighted and the bound GDP molecule is shown in its VdW surface representation colored gray.

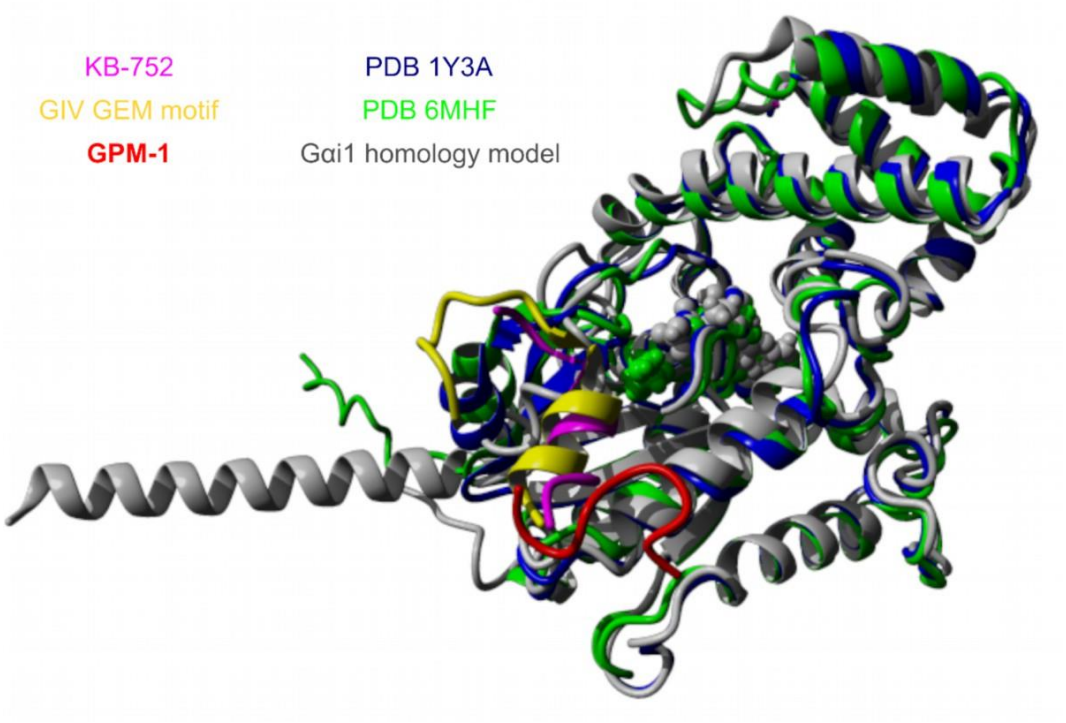

Figure S11. The Fig. shows the structural alignment between two X-ray crystallographic structures of Gαi namely, (chain B of) PDB 1Y3A[33] (blue cartoon) bound to the GDP-selective peptide KB-752 (pink cartoon), PDB 6MHF[40] (green cartoon), bound to the GDP-selective GEM-peptide derived from GIV (yellow cartoon), and the homology model of Gαi (gray cartoon and molecular surface) created in this study with the molecular docking-generated bound conformation of **GPM-1** (red cartoon). The backbone alignment between three structures had an RMSD of 1.63 Å over 285 aligned residues with 99.30% sequence identity. The overlapping positioning of the bound conformations of KB-752 (pink cartoon), GIV (yellow cartoon), and **GPM-1** (red cartoon) indicate that all three peptides bind to a very similar region on Gαi.

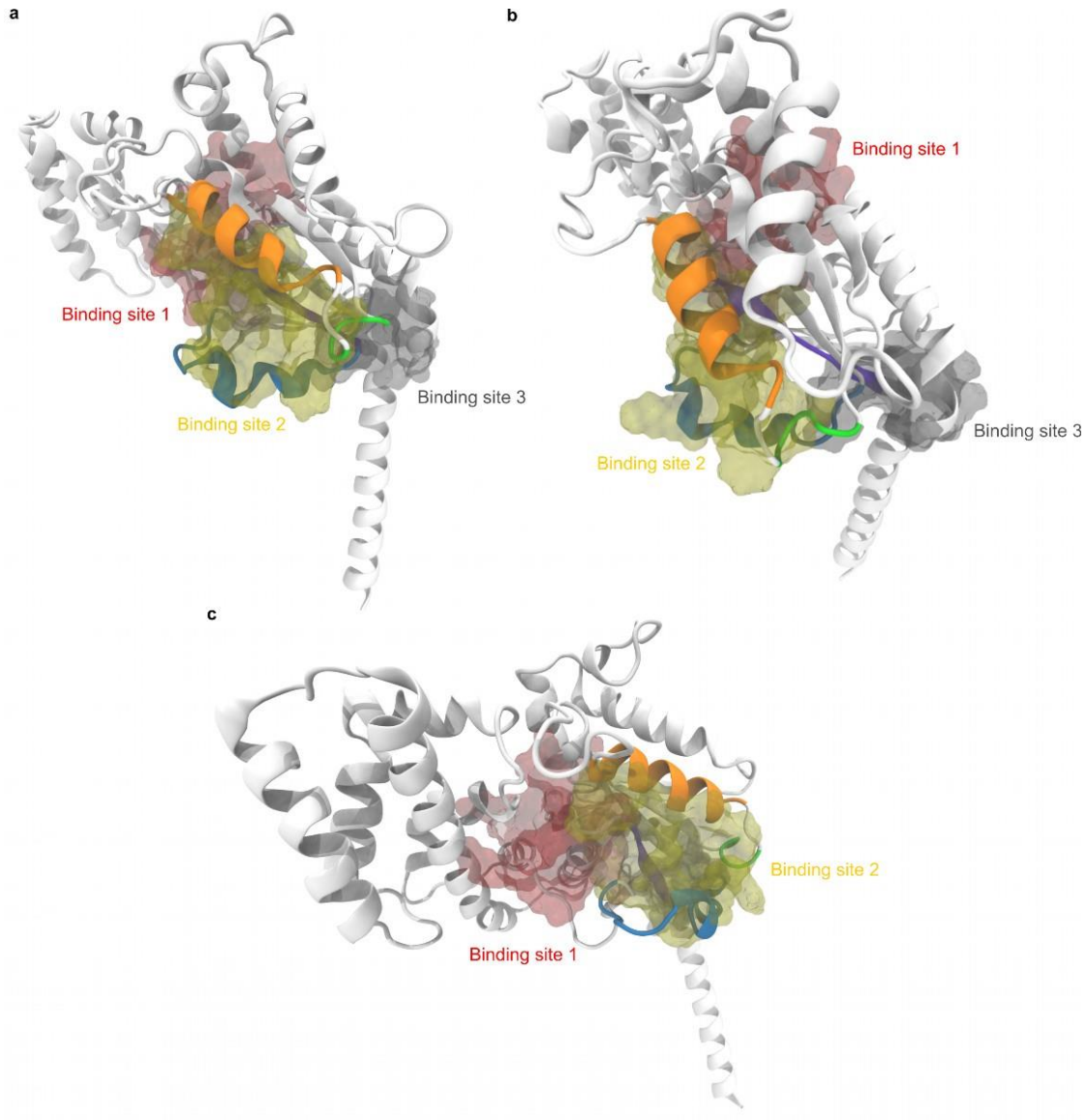

Figure S12. Computationally predicted binding sites on Gαi. The Fig. shows the three major binding sites predicted by the DoGSiteScorer[15,16] algorithm used via SeeSAR (version 10.1, www.biosolveit.de/SeeSAR). The experimentally determined GDP binding site on Gαi was correctly predicted, shown as binding site 1 (red surface containing 35 residues). A second binding site (yellow surface containing 21 residues) predicted here eventually turned out to be the best binding site for the peptides used in this study as determined by independent docking simulations. A third binding site (gray surface comprising of 15 residues) to which the best binding peptide **GPM-3** anchored its C-terminal residues facilitating proper binding to Gαi. Panel **a** shows the Gαi structure oriented to Fig. S10 as reference, panel **b** shows a top view of the protein making all three predicted binding sides visibly oriented, while panel **c** shows a side view of the protein focusing on predicted binding sites 1 and 2 overlapping each other's molecular surfaces. This visualization is an indicator that peptide binding to binding site 2 will have a consequent effect on binding site 1 that houses the GDP molecule.

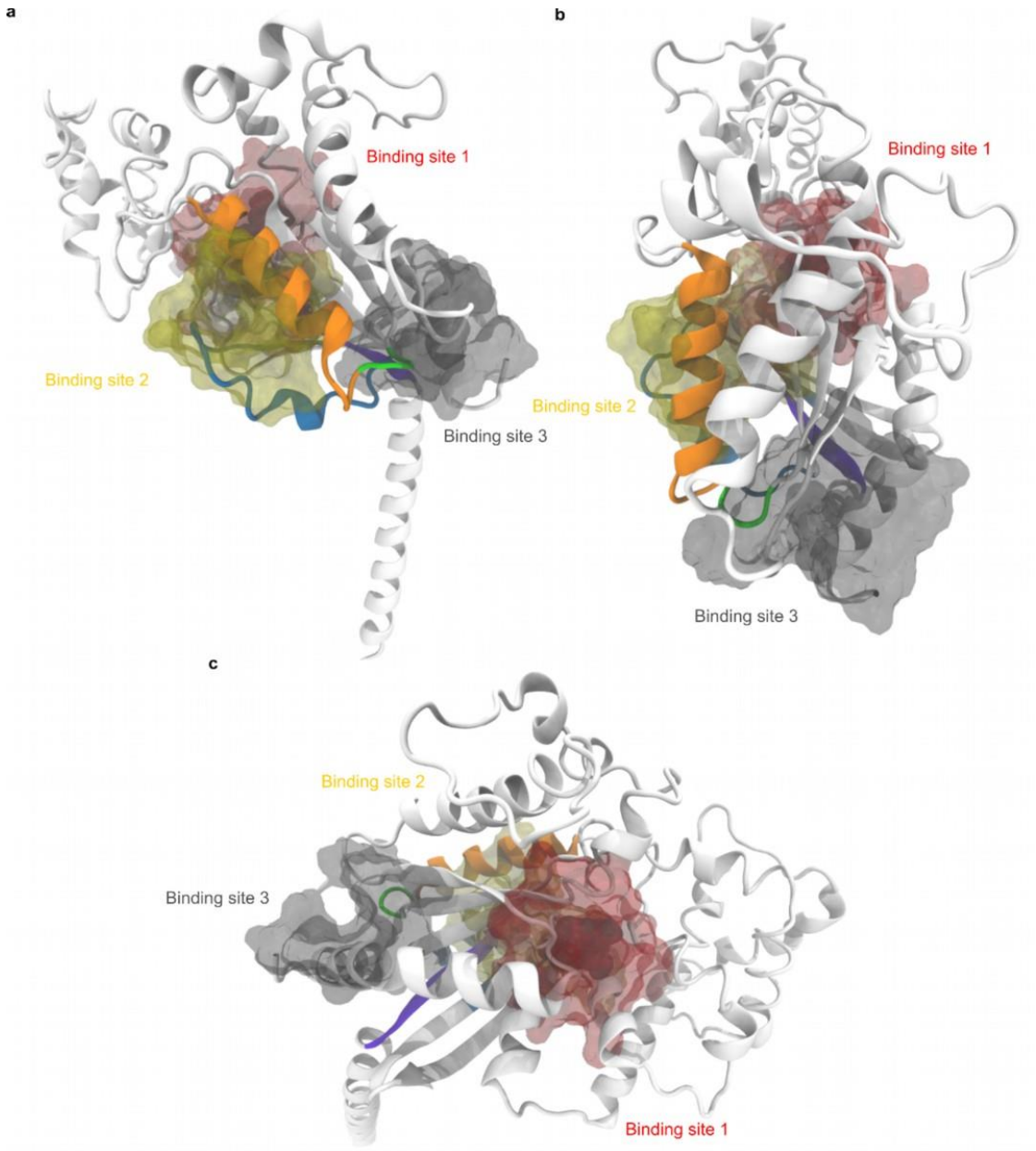

Figure S13. Computationally predicted binding sites on Gαs. The Fig. shows the three major binding sites on (PDB 6EG8[14] – Chain I) Gαs, predicted by the DoGSiteScorer[15,16] algorithm used via SeeSAR (version 10.1, www.biosolveit.de/SeeSAR). The experimentally determined GDP binding site on Gαs was correctly predicted, shown as binding site 1 (red surface containing 29 residues). A second binding site (yellow surface containing 27 residues) predicted here eventually turned out to be the best binding site for the peptides used in this study as determined by independent docking simulations. A third binding site (gray surface comprising of 17 residues) to which the peptide **GPM-1 Y5A** bound was also predicted. Panels **a, b and c** show different orientations of the protein to reveal the fact that there is a large overlap between the residues of binding site 1 and 2. This visualization is an indicator that peptide binding to binding site 2 will have a consequent effect on binding site 1 that houses the GDP molecule.

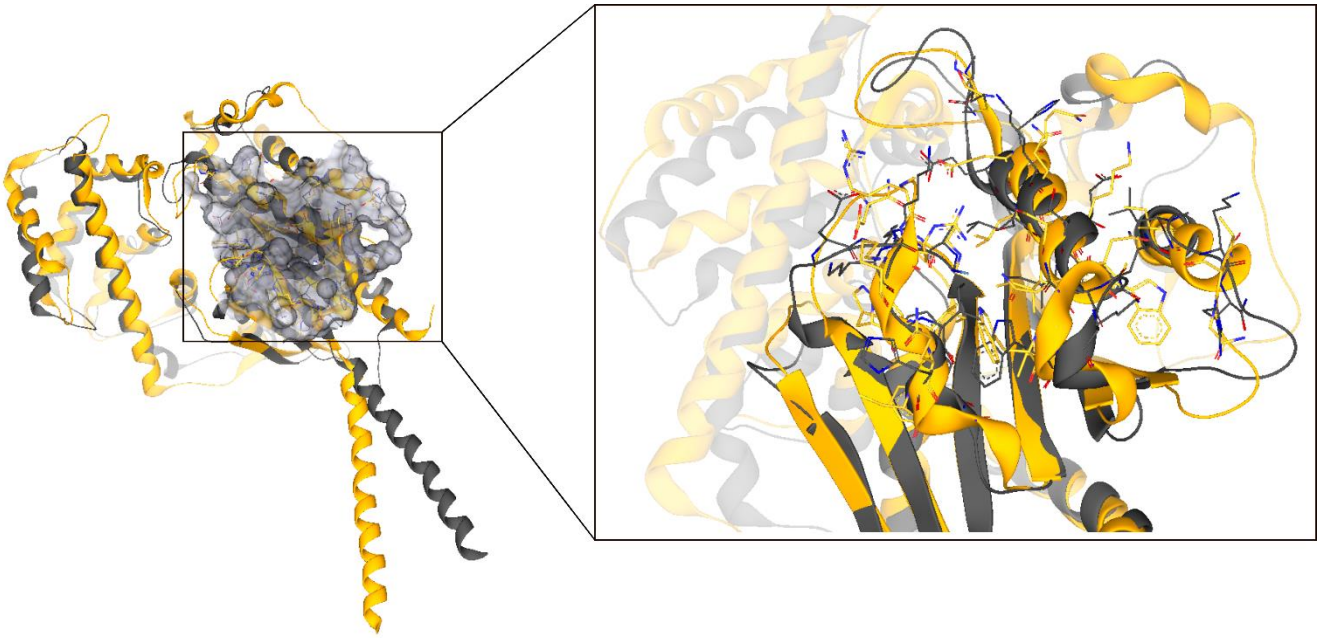

Figure S14. Structural alignment of the Gαi homology model and Gαs. The Fig. shows the structural alignments between the Gαi homology model used in the current study (grey) and the Gαs subunit (orange) extracted from the X-ray crystallographic structure of the GDP-bound Gαs heterotrimer (PDB 6EG8[14] – Chain I). The **GPM-1** binding site was isolated (transparent grey surface) on the homology model used as the basis of the structural alignment in SeeSAR. The alignment indicates an overall 0.8 Å RMSD between 26 aligned residues between the binding sites of the two structures and an overall RMSD of 1.42 Å over 291 aligned residues with 43% sequence identity.

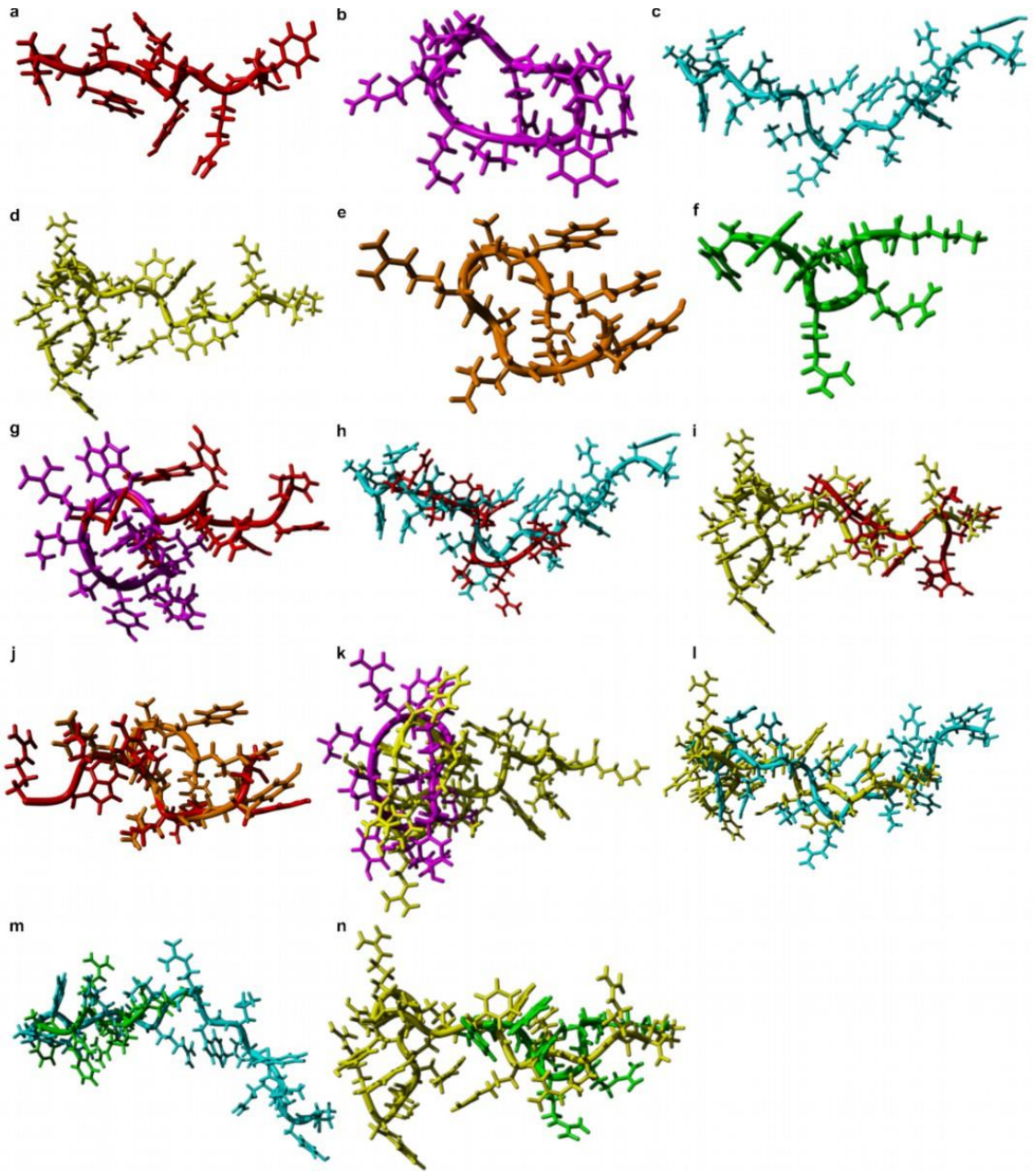

Figure S15. Computationally designed peptide structures and structural alignments. The Fig. shows the final snapshots of the 100 ns MD simulation of the peptides **GPM-1** (red, **a**), **GPM-1b** (magenta, **b**), **GPM-1c** (cyan, **c**), **GPM-1d** (yellow, **d**), **GPM-1 Y5A** (orange, **e**) and, peptide **15** (green, **f**) which are used as inputs for molecular docking simulations. Panels **g-n** show structural alignments between **GPM-1** and **GPM-1b** (panel **g**), **GPM-1** and **GPM-1c** (panel **h**), **GPM-1** and **GPM-1d** (panel **i**), **GPM-1** and **GPM-1 Y5A** (panel **j**) **GPM-1b** and **GPM-1d** (panel **k**), **GPM-1c** and **GPM-1d** (panel **l**), peptide **15** and **GMP-1c** (panel **m**), peptide **15** and **GMP-1d** (panel **n**). All structural alignments were done using the MUSTANG algorithm[31-33,35-36,38-39].

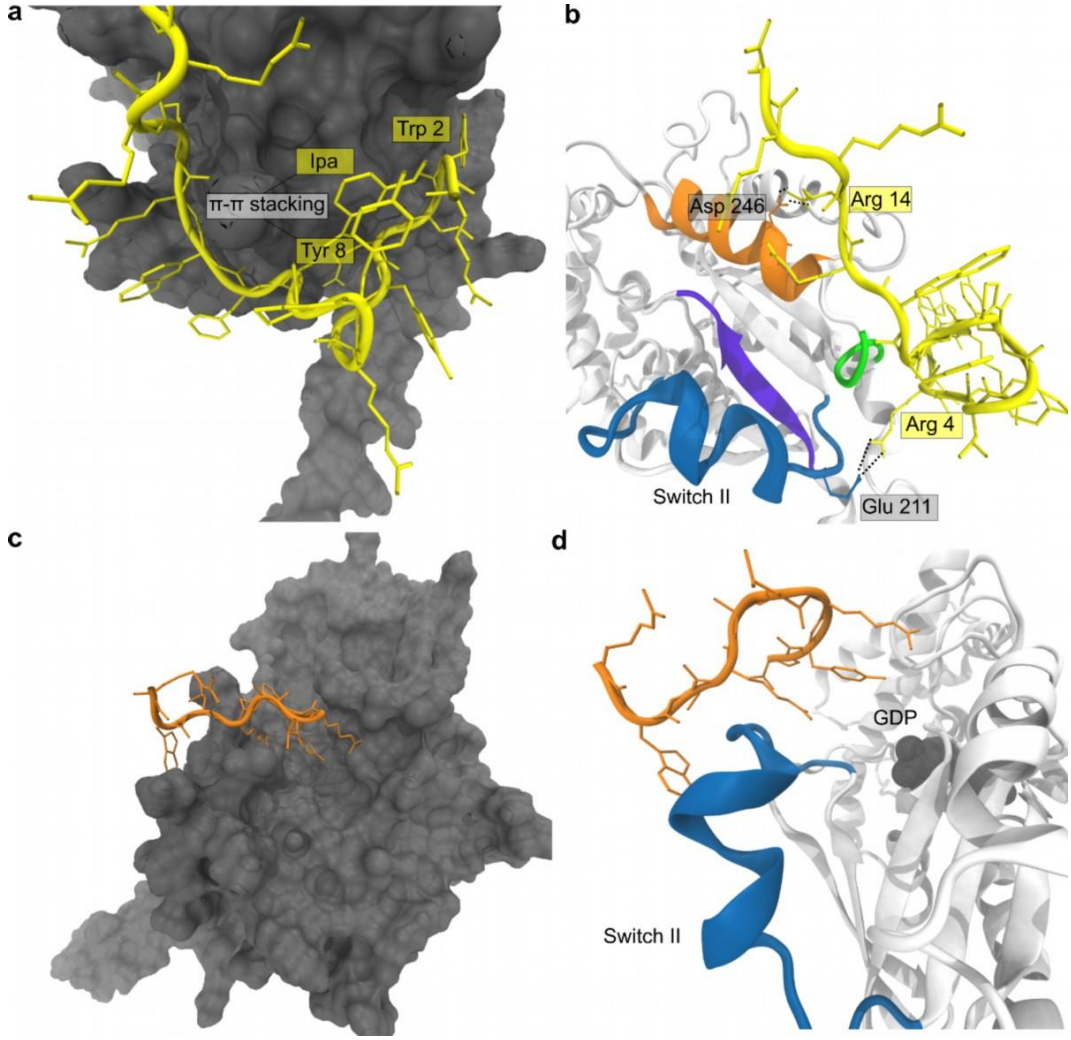

Figure S16. Computational analyses of Gαi-peptide interactions. a, **c**: molecular surface (gray) of Gαi on which **GPM-1d** (yellow, **a**) and **GPM-1 Y5A** (orange, **c**) are bound respectively. In **a**, the side chains involved in hydrophobic interactions with Gαi and intramolecular π-π-stacking interactions are labeled. **b**: Gαi structure (white cartoon) with Switch II (blue), α3 (orange), β1 (violet), and α3-β5 loop (green) depicted. The bound conformation of **GPM-1d** (yellow), with the hydrogen bonding (black sticks) partners labeled. **d:** in simulation, **GPM-1 Y5A** (orange) dissociates from its initial bound state and is found close to the Switch II region (blue), held only by long electrostatic interactions, and no hydrogen bonds are observed.

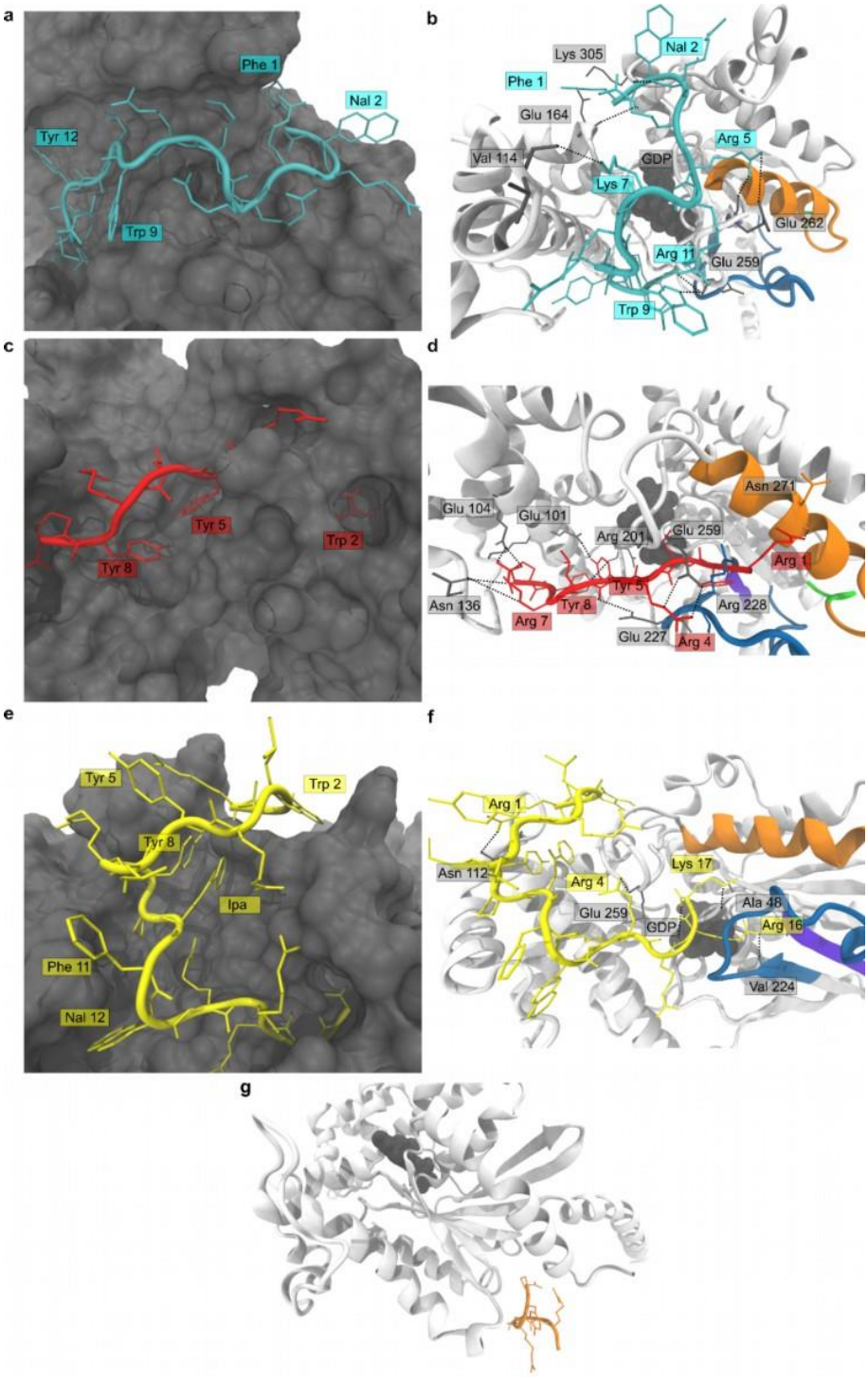

Figure S17. Computational analyses of Gαs-peptide interactions. **a**, **c**, **e**: molecular surface (gray) of Gαs on which **GPM-1c** (cyan, **a**), **GPM-1** (red, **c**) and **GPM-1d** (yellow, **e**) are bound respectively. The side chains involved in hydrophobic interactions with Gαs and intramolecular π-π-stacking interactions are labeled. In panels **b**, **d**, **f**, **g**, the protein Gαs is shown as a white cartoon with the different structural elements color coded as follows: Switch II (blue), α3 (orange), β1 (violet), and α3-β5 loop (green), and the GDP molecule shown as gray spheres. In the panels **b**, **d**, **f**, the bound conformations of **GPM-1c** (cyan, **b**), **GPM-1**(red, **d**), and **GMP-1d** (yellow, **f**) are shown with the residues involved in H-bonded interactions (black dotted lines) marked and labeled. Panel **g** shows the full Gas protein as a white cartoon and (un)bound conformation of **GPM-1 Y5A** shown to explain that it has been dislodged from its bound state during the course of the simulation.

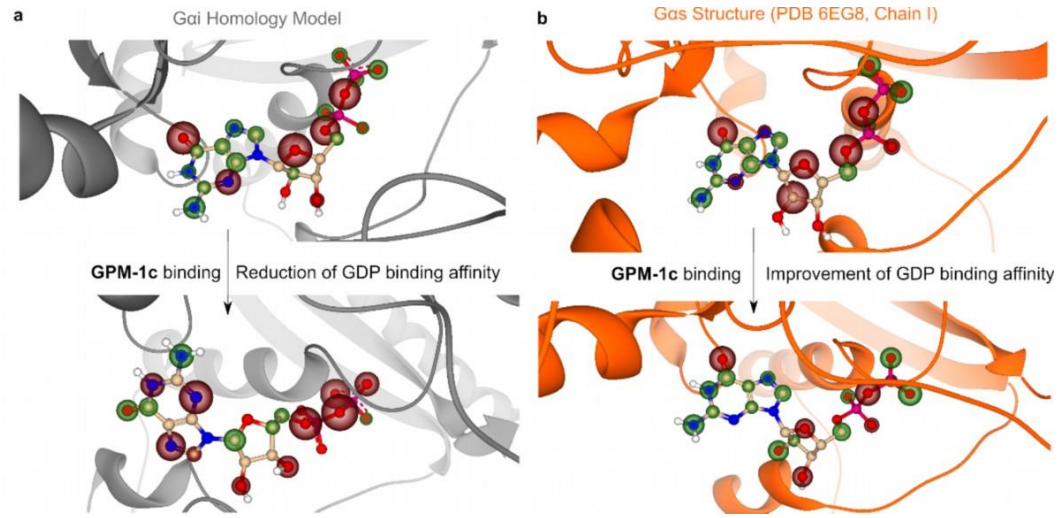

Figure S18. Visual assessment of change in GDP binding affinity upon GPM-1c binding to Gαi and Gαs. The figure represents a visual assessment of the change in GDP binding affinity for the most active peptide (**GPM-1c**) binding to Gαi (panel **a**) and Gαs (panel **b**). The GDP molecule is represented as beige sticks with the atomic contributions to binding affinities computed by the HYDE scoring function[36,40] in the molecular modeling program SeeSAR. A visual representation of the affinities is shown as translucent spheres (HYDE Coronas, https://www.biosolveit.de/products/#HYDE). Green coronas represent positive contributions to the binding affinities while red coronas denote unfavorable contributions determined based on the contribution of H-bonding and desolvation energies to the binding affinity. The size of the coronas is proportional to the underlying HYDE energy values. In **a** (Gαi, gray cartoons), the binding of **GPM-1c** results in the reduction of GDP binding affinity deduced from the increase in the number of red coronas relating to unfavorable atomic interactions, while in **b** (Gαs, orange cartoon), the opposite is observed, i.e., the reduction in the number of red coronas indicating an improvement in the GDP binding affinity. In both **a** and **b** the top structure denotes the initial structure and the lower part denotes the MD snapshot at 50ns. This is an additional visual representation supplementing the numeric MMPBSA binding energies extracted from the MD trajectories as furnished in Tables S11 and S12.

6. Supporting Tables

Table S1. Hit sequences of all 101 identified hits of the one-bead-one-compound (OBOC) library screening.

No.	-4	-3	-2	-1	0	+1	+2	+3	+4	No.	-4	-3	-2	-1	0	+1	+2	+3	+4
1	A	T	G	H	Y	K	Q	Y	D	52	W	W	P	G	H	R	F	I	A
2	K	V	R	M	Y	E	E	I	E	53	T	R	P	W	H	H	R	M	A
3	Y	K	K	R	Y	Y	G	G	F	54	F	T	G	N	H	A	L	Q	D
4	I	K	F	P	Y	R	R	M	F	55	Y	D	G	R	H	L	R	P	E
5	D	W	N	R	Y	V	G	F	G	56	G	R	A	F	H	S	Y	P	E
6	N	W	A	H	Y	V	A	I	G	57	N	W	Q	N	H	P	F	A	G
7	A	W	L	S	Y	Y	H	N	G	58	F	K	H	N	H	A	S	F	G
8	P	K	A	T	Y	T	Q	R	G	59	Q	W	K	H	H	W	Y	Q	G
9	R	K	S	W	Y	L	F	A	H	60	G	F	W	R	H	P	Y	R	G
10	P	K	K	T	Y	R	W	A	H	61	M	Y	Y	Y	H	K	V	R	H
11	W	G	R	S	Y	S	H	P	H	62	M	Y	Y	Y	H	K	V	R	H
12	Q	T	A	Y	Y	F	K	Q	H	63	R	A	R	T	H	F	W	I	I
13	A	H	D	T	Y	R	F	G	I	64	Q	R	Y	L	H	L	L	R	I
14	W	P	K	N	Y	R	Q	K	I	65	F	H	Q	W	H	R	T	Q	K
15	W	P	F	A	Y	T	K	N	I	66	M	A	T	Y	H	P	Y	Q	K
16	F	D	P	S	Y	F	R	N	I	67	N	W	Q	A	H	V	V	S	K
17	G	P	Y	G	Y	S	W	R	I	68	E	T	L	H	H	P	V	V	K
18	N	M	M	V	Y	H	R	K	K	69	P	M	M	A	H	M	S	G	L
19	Y	Y	E	K	Y	T	R	T	K	70	M	N	L	Y	H	F	D	H	L
20	D	F	I	A	Y	A	N	W	K	71	R	R	L	V	H	H	R	V	L
21	P	I	A	R	Y	A	R	W	K	72	S	S	M	F	H	I	G	L	N
22	N	W	G	A	Y	L	D	G	L	73	F	K	N	P	H	P	Y	N	N
23	N	W	G	A	Y	L	D	G	L	74	H	K	E	M	H	S	E	I	M
24	P	H	W	M	Y	I	D	I	L	75	R	I	N	W	H	G	G	N	M
25	N	F	I	R	Y	A	H	K	L	76	R	K	W	T	H	D	G	R	M
26	W	F	Q	S	Y	W	G	N	L	77	L	M	D	Y	H	F	R	R	M
27	R	K	A	S	Y	I	H	Q	N	78	Q	R	A	R	H	D	S	F	Q
28	S	W	T	M	Y	P	F	R	N	79	I	R	Q	H	H	K	T	T	Q
29	T	F	D	R	Y	T	A	L	M	80	V	R	V	Y	H	H	N	G	R
30	Q	L	K	A	Y	V	A	S	M	81	S	S	H	V	H	K	F	M	R
31	Q	A	N	H	Y	M	W	Y	M	82	W	P	Y	D	H	R	F	M	R
32	V	L	K	F	Y	E	F	G	P	83	Q	M	F	S	H	M	H	P	R
33	G	E	P	R	Y	F	K	Y	P	84	P	D	R	D	H	H	K	Y	R
34	R	W	L	R	Y	L	R	Y	P	85	K	D	G	L	H	R	V	Y	R
35	S	I	N	Y	Y	F	S	M	Q	86	T	S	R	Y	H	M	H	R	I

36	F	S	R	R	Y	R	S	P	Q	87	W	V	Q	R	H	P	Y	A	V
37	S	Y	M	D	Y	F	H	A	R	88	W	F	Q	A	H	K	F	L	V
38	H	H	Y	N	Y	R	Y	T	R	89	P	M	R	G	H	I	M	Q	V
39	F	A	N	G	Y	R	W	Y	R	90	P	F	R	S	H	V	S	W	V
40	H	F	F	Y	Y	D	Q	Q	S	91	F	L	G	W	H	L	G	N	W
41	Q	I	L	K	Y	Y	N	F	T	92	V	T	I	P	H	W	S	M	W
42	N	W	I	K	Y	L	G	K	T	93	R	Y	H	I	H	E	Y	H	Y
43	D	G	G	G	Y	R	S	K	T	94	I	H	W	T	H	H	H	K	Y
44	W	P	S	H	Y	R	K	Q	T	95	H	E	W	V	H	G	F	L	Y
45	Y	L	K	H	Y	H	S	A	V	96	K	R	R	T	H	A	H	P	Y
46	R	H	D	H	Y	N	A	Y	V	97	K	K	S	K	H	P	W	R	Y
47	N	T	K	Q	Y	S	S	A	Y	98	R	Q	P	Y	C	P	Y	H	W
48	R	P	L	L	Y	H	K	I	Y	99	Y	Y	N	V	C	H	G	I	L
49	Q	D	H	P	Y	A	Q	K	Y	100	D	S	I	G	C	F	N	Q	F
50	N	W	R	N	Y	V	A	L	Y	101	F	Q	Y	Q	C	R	K	H	F
51	R	H	D	D	Y	S	Y	Q	D										

M = norleucine, as used in an earlier study[37].

Table S2. Multiple sequence alignment by Clustal Omega (O 1.2.4)[41] of the 13 selected screening-derived hits.

peptide				Φ	ζ	W	Φ	[+/-]	Ω	Φ					
1	-	-	-	-	R	**W**	**L**	**R**	**Y**	**L**	R	Y	P	-	-
2	-	-	-	-	**N**	**W**	G	A	**Y**	**L**	D	G	L	-	-
7	-	-	-				**F**	Q	**Y**	Q	C	R	K	H	F
10		S	S	**M**	F	H	**I**	G	L	N	-	-	-	-	-
3	-	-	-	-	**N**	F	**I**	**R**	**Y**	A	H	K	L	-	-
4	-	-	-	-	-	**W**	P	**K**	N	**Y**	R	Q	K	I	-
12	-	-	-	-	**Q**	I	**L**	**K**	**Y**	**Y**	N	F	T	-	-
11	-	K	V	R	M	Y	E	**E**	I	E	-	-	-	-	-
9	-	-	M	**Y**	Y	Y	H	**K**	V	R	H	-	-	-	-
5	-	-	-	-	-	**W**	**V**	Q	R	H	P	Y	A	V	-
6	-	-	F	H	**Q**	**W**	H	**R**	T	Q	K	-	-	-	-
8	T	S	R	**Y**	H	M	H	**R**	I	-	-	-	-	-	-
13	-	P	D	R	D	H	H	**K**	**Y**	R	-	-	-	-	-

Symbols according to Aasland et al.[3] grouped as follows: Φ: hydrophobic (V, I, L, F, W, Y, M); Ω: aromatic (F, W, Y); Ψ: large aliphatic (V, I, L, M); π: small (P, G, A, S); ζ: uncharged hydrophilic (N, Q, S, T); [+]: basic (H, K, R) and [-]: acidic amino acids (D, E). The residues of the screening-derived peptides which match the ΦζWΦ[+/-]ΩΦ-motif are shown in bold letters. The first four peptides (**1**, **2**, **7**, **10**) showed binding towards Gαi1·GDP. M = norleucine (Nle)[37].

Table S3. Analytical characterization of peptides prepared in this study.

No.	Peptide sequence	Mw (Mw theor.)	HPLC C18 t_R (min)	HPLC C8 t_R (min)
GPM-1	RWLRYLRYP	1321.73[a] (1320.76)	31.63[d]	22.72[e]
GPM-1 Y5A	RWLRALRYP	1229.74[a] (1228.73)	30.30[d]	25.99[e]
GPM-1b	cyc[KRWLRYLRYP]	1432.88[c] (1431.83)	34.27[d]	15.23[h]
GPM-1c	F(2Nal)RRRRKRWLRYLRYP	2418.40[c] (2417.41)	34.52[d]	14.80[h]
GPM-1d	cyc[RWLRYLRYP]F(2Nal)RRRRK	2634.50[c] (2633.46)	39.44[d]	20.13[j]
2	NWGAYLDGL	1007.49[a] (1006.49)	16.17[h]	15.75[h]
3	NFIRYAHKL	1160.66[a] (1159.66)	18.70[e]	18.35[e]
4	WPKNYRQKI	1231.71[a] (1230.70)	15.15[f]	14.66[f]
5	WVQRHPYAV	1154.62[a] (1153.61)	15.28[f]	15.04[f]
6	FHQWHRTQK	1266.66[c] (1265.65)	22.05[g]	21.44[g]
7	FQYQCRKHF	1255.61[a] (1254.61)	15.58[f]	15.27[f]
8	TSRYHMHRI	1181.71[c] (1180.66)	14.90[f]	14.68[f]
9	MYYYHKVRH	1277.65[c] (1276.68)	14.08[f]	13.93[f]
10	SSMFHIGLN	493.77[b] (985.53)	14.66[h]	14.64[h]
11	KVRMYEEIE	1177.66[c] (1176.65)	19.16[e]	18.93[e]
12	QILKYYNFT	1188.65[a] (1187.63)	21.85[e]	21.58[e]
13	PDRDHHKYR	1222.57[c] (1221.61)	16.31[i]	15.38[i]
14	KRWLRYLRYP	1449.89[c] (1448.85)	30.92[d]	21.82[e]
15	F(2Nal)RRRRK	1114.69[c] (1113.68)	25.99[d]	16.79[f]
KB-752[42]	H-SRVTWYDFLMEDTKSR-OH	2034.00[c] (2032.97)	36.71[d]	17.58[h]

M = norleucine, as used in an earlier study[37]. All peptides were synthesized as acid amides unless otherwise stated. Mass peaks were detected as a) $[M+H]^+$ and b) $[M+2H]^{2+}$ with LC-ESI-MS and as c) $[M+H]^+$ with MALDI-MS. For analytical RP-HPLC the following gradients were used: d) 0 – 60% eluent B in 60 min, e)10 – 50% eluent B in 40 min, f) 10 – 40% eluent B in 30 min, g) 0 – 40% eluent B in 40 min, h) 20 – 50% eluent B in 30 min, i) 0 – 30% eluent B in 30 min and j) 20 – 60% eluent B in 40 min. *All peptides were >98% HPLC pure.

Table S4. Analytical characterization of peptides prepared in this study.

No.	Peptide sequence	Mw (Mw theor.)	HPLC C18 t_R (min)
Cf-**GPM-1**	Cf-RWLRYLRYP	1679.79[c] (1678.80)	22.82, 23.25[g]
Cf-**GPM-1 Y5A**	Cf-RWLRALRYP	794.40[b] (1586.78)	39.80, 40.19[d]
FITC-**GPM-1b**	cyc[K(FITC)RWLRYLRYP]	1821.83[c] (1820.86)	42.75[d]
Cf-**GPM-1c**	Cf-F(2Nal)RRRRKRWLRYLRYP	2776.37[c] (2775.46)	41.12[d]
FITC-**GPM-1d**	cyc[RWLRYLRYP]F(2Nal)RRRRK(FITC)	3023.64[c] (3022.50)	42.56[d]
Cf-**2**	Cf-NWGAYLDGL	1365.53[a] (1364.54)	21.81, 22.58[g]
Cf-**3**	Cf-NFIRYAHKL	759.86[b] (1517.71)	19.24, 20.09[g]
Cf-**4**	Cf-WPKNYRQKI	1589.78[c] (1588.75)	16.09, 17.46[g]
Cf-**5**	Cf-WVQRHPYAV	1512.65[a] (1511.66)	18.08, 19.18[g]
Cf-**6**	Cf-FHQWHRTQK	1624.69[a] (1623.70)	15.46, 16.44[f]
Cf-**7**	Cf-FQYQCRKHF	1613.67[a] (1612.66)	17.36, 18.24[g]
Cf-**8**	Cf-TSRYHMHRI	1539.70[a] (1538.71)	13.11, 13.86[f]
Cf-**9**	Cf-MYYYHKVRH	818.37[b] (1634.73)	17.33, 18.76[g]
Cf-**10**	Cf-SSMFHIGLN	1344.58[a] (1343.58)	22.62, 23.70[g]
Cf-**11**	Cf-KVRMYEEIE	1535.78[c] (1534.70)	17.81, 18.27[g]
Cf-**12**	Cf-QILKYYNFT	773.85[b] (1545.68)	22.47, 23.24[g]
Cf-**13**	Cf-PDRDHHKYR	790.83[b] (1579.66)	18.66, 19.20[e]
Cf-**14**	Cf-KRWLRYLRYP	1807.91[c] (1806.90)	18.71, 19.63[f]
Cf-**15**	Cf-F(2Nal)RRRRK	1472.73[c] (1471.73)	18.32, 18.99[f]
Cf-KB-752	Cf-SRVTWYDFLMEDTKSR-OH	2392.11[c] (2391.02)	41.29[d]
Btn-**GPM-1**	RWLRYLRYP-O2Oc-K(Biotin)	1821.08[c] (1820.00)	32.95[d]
Btn-**GPM-1c**	F(2Nal)RRRRK(PEG_4-Biotin)RWLRYLRYP	2891.70[c] (2890.63)	35.93[d]
Btn-**GPM-1d**	cyc[RWLRYLRYP]F(2Nal)RRRRK(PEG_4-Biotin)	3107.72[c] (3106.68)	40.09[d]
Btn-**GPM-15**	F(2Nal)RRRR-O2Oc-K(Biotin)	1485.85[c] (1484.83)	28.63[d]

M = norleucine, as used in an earlier study[37]. All peptides were synthesized as acid amides unless otherwise stated. Mass peaks were detected as a) $[M+H]^+$ and b) $[M+2H]^{2+}$ with LC-ESI-MS and as c) $[M+H]^+$ with MALDI-MS. For analytical RP-HPLC the following gradients were used: d) 0 – 60% eluent B in 60 min, e) 10 – 50% eluent B in 40 min, f) 20 – 50% eluent B in 30 min, g) 20 – 60% eluent B in 40 min. *All peptides were >98% HPLC pure.

Table S5. Validations of homology model from Swiss Model Software.

All-Atoms contacts	Clash score, all atoms		1.25	100thpercentile# (N=773, 1.90Å ± 0.25 Å
	Clash score is the number of serious steric overlaps (> 0.4 Å) per 1000 atoms			
Protein geometry[a]	Poor rotamers	2	0.67%	Goal: <0.3%
	Favored rotamers	293	97.67%	Goal: >98%
	Ramachandran outliers	0	0.00%	Goal: <0.05%
	Ramachandran favored	342	98.56%	Goal: >98%
	Rama distribution Z-score	-0.65 ± 0.44		Goal: abs(z-score) <2
	MolProbity score	0.85		100thpercentile# (N=12147,1.90 Å ± 0.25 Å)
	Cβ deviations>0.25 Å	0	0.00%	Goal:0
	Bad bonds:	5/2875	0.17%	Goal: 0%
	Bad angles:	5/3873	0.13%	Goal: < 0.1%
Peptide omegas	Cis Proline	0/3	0.00%	Expected: ≤ 1 per chain, or ≤ 5%

[a] The left column gives the raw count, right column gives the percentage, combine clash score, rotamer and Ramachandran evaluations of homology model. 100thpercentile# is the best among structures of comparable resolutions, othpercentile is the worst. Color codes (Green: favored, yellow: moderate, red: unfavored).

Table S6. Homology model energy profile calculations.

Total amino acids with high energy	9	percentage	2.58
Total number of amino acids	349	Total numbers of atoms	2799
Total number of non-local atomic interactions	45538	Non-local normalized energy Z-score	-0.61
Total non-local energy of the protein (E/KT units)	-2996		

Table S7. Structural alignments of the **GPM-1**-derived peptides and peptide **15**.

peptide	**GPM-1b**	**GPM-1c**	**GPM-1d**	**GPM-1 Y5A**
GPM-1	3.44 Å between 9 aligned residues	2.94 Å between 9 aligned residues	4.13 Å over 9 aligned residues	0.29 Å between 4 aligned residues
GPM-1b	-	n.d.	2.50 Å between 9 aligned residues	n.d.
GPM-1c	n.d.	-	0.98 Å between 6 aligned residues	n.d.
15	n.d.	2.64 Å between 7 aligned residues	2.71 Å between 7 aligned residues	n.d.

n.d.: not determined

Table S8. Comparison between binding energy calculations predicted by VINA[13] and PRODIGY[17] for two best poses for each peptide in the Gαi docked complexes.

peptide	Binding Energy Vina pose1 (KJ mol^{-1})	Binding Energy Vina pose2 (KJ mol^{-1})	Binding Energy PRODIGY pose1 (KJ mol^{-1})	Binding Energy PRODIGY pose2 (KJ mol^{-1})
GPM-1	-31.80	-34.10	-45.61	-43.10
GPM-1 Y5A	-30.39	-32.21	-42.16	-40.21
GPM-1b	-24.69	-33.18	-37.66	-38.49
GPM-1c	-26.23	-30.84	-47.70	-60.25
GPM-1d	-27.15	-29.33	-43.51	-46.44
14	-28.45	-33.51	-41.00	-41.00
15	-31.13	-34.90	-38.07	-36.82
KB-752	-26.61	-30.08	-39.75	-40.58

Table S9. Comparison between binding energy calculations predicted by VINA[13] and PRODIGY[17] for two best poses for each peptide in the Gαs docked complexes.

peptide	Binding Energy Vina pose1 (KJ mol^{-1})	Binding Energy Vina pose2 (KJ mol^{-1})	Binding Energy PRODIGY pose1 (KJ mol^{-1})	Binding Energy PRODIGY pose2 (KJ mol^{-1})
GPM-1	-27.48	-26.25	-43.11	-41.40
GPM-1 Y5A	-29.56	-31.78	-42.32	-43.75
GPM-1c	-36.41	-37.66	-48.63	-49.65
GPM-1d	-34.32	-33.17	-45.48	-44.12

Table S10. Mean Backbone RMSD comparison table for MD simulation of Gαi/s-bound and unbound peptides from their respective 50 ns MD simulation.

Peptide	Mean backbone RMSD (Å)		
	RMSD unbound (Å)	RMSD Gαi-bound (Å)	RMSD Gαs-bound (Å)
GPM-1	3.44 ± 1.20	3.42 ± 0.98	2.12 ± 0.64
GPM-1 Y5A	3.66 ± 1.75	2.99 ± 0.82	2.73 ± 1.47
GPM-1b	1.19 ± 0.20	3.11 ± 0.82	n.d.
GPM-1c	6.23 ± 1.50	3.21 ± 0.81	2.71 ± 1.11
GPM-1d	3.90 ± 0.60	2.79 ± 0.66	2.39 ± 0.46
15	1.96 ± 0.60	2.13 ± 0.42	n.d.

n.d.: not determined.

Table S11. Mean MMPBSA binding energies calculated to quantify the interaction between each peptide and Gαi as well as the interaction between GDP and Gαi when a particular peptide is bound.

Peptide	Mean MMPBSA energy (kJ mol^{-1})	
	Peptide-Gαi (kJ mol^{-1})	GDP-Gαi (kJ mol^{-1})
GPM-1	-300.23	286.27
GPM-1 Y5A	-401.87	158.65
GPM-1b	-497.82	318.34
GPM-1c	67.56	-436.38
GPM-1d	30.34	-433.67
15	-512.17	309.67
N/A	N/A	-306.23

The last row shows the binding energy of GDP on the Gαi homology model. More positive values for binding energies indicate better binding.

Table S12. Mean MMPBSA binding energies calculated to quantify the interaction between each peptide and Gαs as well as the interaction between GDP and Gαs when a particular peptide is bound.

Peptide	Mean MMPBSA energy (kJ mol^{-1})	
	Peptide-Gαs (kJ mol^{-1})	GDP-Gαs (kJ mol^{-1})
GPM-1	110.53	166.73
GPM-1 Y5A	-413.45	-198.12
GPM-1c	288.24	332.78
GPM-1d	192.74	246.87
N/A	N/A	-248.12

The last row shows the binding energy of GDP to Gαs. More positive values for binding energies indicate better binding.

7. Supporting Video Description

Video S1: MD simulation of GPM-1 bound to Gαi. The movie shows the recording of a 50 ns MD simulation trajectory of **GPM-1** bound to Gαi. **GPM-1** is depicted in red while the structure of Gαi is in gray cartoons. A VdW spheres representation of the bound GDP molecule is also displayed. Secondary structures are dynamically updated using the STRIDE algorithm[43]. 2000 frames from the raw trajectory were subjected to a smoothing factor of 5 to generate the movie.

Video S2: MD simulation of GPM-1b bound to Gαi. The movie shows the recording of a 50 ns MD simulation trajectory of **GPM-1b** bound to Gαi. **GPM-1b** is depicted in magenta while the structure of Gαi is in gray cartoons. A VdW spheres representation of the bound GDP molecule is also displayed. Secondary structures are dynamically updated using the STRIDE algorithm[43]. 2000 frames from the raw trajectory were subjected to a smoothing factor of 5 to generate the movie.

Video S3: MD simulation of GPM-1c bound to Gαi. The movie shows the recording of a 50 ns MD simulation trajectory of **GPM-1c** bound to Gαi. **GPM-1c** is depicted in cyan while the structure of Gαi is in gray cartoons. A VdW spheres representation of the bound GDP molecule is also displayed. Secondary structures are dynamically updated using the STRIDE algorithm[43]. 2000 frames from the raw trajectory were subjected to a smoothing factor of 5 to generate the movie.

8. References

1 M. C. Sweeney, A.-S. Wavreille, J. Park, J. P. Butchar, S. Tridandapani, D. Pei, *Biochemistry* 2005, **44**, 14932-14947.
2 M. C. Sweeney, D. Pei, *J. Comb. Chem.* 2003, **5**, 218-222.
3 R. Aasland, C. Abrams, C. Ampe, L. J. Ball, M. T. Bedford, G. Cesareni, M. Gimona, J. H. Hurley, T. Jarchau, V. P. Lehto, et al., *FEBS letters* 2002, **513**, 141-144.
4 B. Nubbemeyer, A. Pepanian, A. A. Paul George, D. Imhof, *ChemMedChem* 2021, **16**, 1697-1716.
5 M. Moreno, E. Giralt, *Toxins* 2015, **7**, 1126-1150.
6 N. A. Lambert, C. A. Johnston, S. D. Cappell, S. Kuravi, A. J. Kimple, F. S. Willard, D. P. Siderovski, *Proc. Natl. Acad. Sci. U. S. A.* 2010, **107**, 7066-7071.
7 D. Goricanec, R. Stehle, P. Egloff, S. Grigoriu, A. Plückthun, G. Wagner, F. Hagn, *Proc. Natl. Acad. Sci. U. S. A.* 2016, 113, E3629-E3638.
8 M.-y. Shen, A. Sali, *Protein Sci.* **2006**, *15*, 2507-2524.
9 F. Melo, D. Devos, E. Depiereux, E. Feytmans, *Proceedings. International Conference on Intelligent Systems for Molecular Biology* 1997, **5**, 187-190.
10 E. Krieger, T. Darden, S. B. Nabuurs, A. Finkelstein, G. Vriend, *Proteins* 2004, **57**, 678-683.
11 J. A. Maier, C. Martinez, K. Kasavajhala, L. Wickstrom, K. E. Hauser, C. Simmerling, *J. Chem. Theory Comput.* 2015, **11**, 3696-3713.
12 E. M. Novoa, L. Ribas de Pouplana, X. Barril, M. Orozco, *J. Chem. Theory Comput* 2010, **6**, 2547-2557.
13 O. Trott, A. J. Olson, *J. Comput. Chem.* 2010, **31**, 455-461.
14 X. Liu, X. Xu, D. Hilger, P. Aschauer, J. K. S. Tiemann, Y. Du, H. Liu. K. Hirata, X. Sun, R. Guixa-Gonzalez, et al., *Cell* 2019, **177**, 1243-1251.
15 A. Volkamer, D. Kuhn, T. Grombacher, F. Rippmann, M. Rarey, *J. Chem. Inf. Model.* 2012, **52**, 360-372.
16 A. Volkamer, A. Griewel, T. Grombacher, M. Rarey, *J. Chem. Inf. Model* 2010, **50**, 2041-2052.
17 A. Varshney, F. P. Brooks, W. V. Wright, IEEE Comput. *Graphics and* Applications 1994, **14**, 19-25.
18 C. A. Johnston, J. K. Ramer, R. Blaesius, Z. Fredericks, V. J. Watts, D. P. Siderovski, *FEBS Lett.* 2005, **579**, 5746-5750.
19 M. M. Bradford, *Anal. Biochem.* 1976, **72**, 248-254.
20 D. Imhof, K. Wieligmann, K. Hampel, D. Nothmann, M. S. Zoda, D. Schmidt-Arras, M. Zacharias, F. D. Böhmer, S. Reissmann, *J. Med. Chem.* 2005, **48**, 1528.
21 H. Ammer, R. Schulz, *FEBS Lett.* 2000, **485**, 157-162.
22 H. Ammer, R. Schulz, *Mol. Pharmacol.* 1997, **52**, 993-999.
23 J. K. Horton, R. C. Martin, S. Kalinka, A. Cushing, J. P. Kitcher, M. J. O'Sullivan, P. M. Baxendale, *J. Immunol. Methods* 1992, **155**, 31-40.
24 R. Reher, T. Kühl, S. Annala, T. Benkel, D. Kaufmann, B. Nubbemeyer, J. P. Odhiambo, P. Heimer, C. A. Bäuml, S. Kehraus, M. Crüsemann, E. Kostenis, D. Tietze, G. M. König, D. Imhof, *ChemMedChem* 2018, **13**, 1634-1643.
25 R. Schrage, A.-L. Schmitz, E. Gaffal, S. Annala, S. Kehraus, D. Wenzel, K. M. Büllesbach, T. Bald, A. Inoue, Y. Shinjo, et al., *Nat. Commun.* 2015, **6**, 10156.
26 R. Schröder, N. Merten, J. M. Mathiesen, L. Martini, A. Kruljac-Letunic, F. Krop, A. Blaukat, Y. Fang, E. Tran, T. Ulven, et al., *J. Biol. Chem.* 2009, **284**, 1324-1336.
27 E. W. K. Seemann, D. Wenzel, R. Schrage, J. Etscheid, T. Bödefeld, A. Bartol, M. Warnken, P. Sasse, J. Klöckner, U. Holzgabe, M. et al., *J. Pharmacol. Ther.* 2017, **360**, 289-299.
28 J. Antony, K. Kellershohn, M. Mohr-Abdrä, A. Kebig, S. Prilla, M. Muth, E. Heller, T. Disingrini, C. Dallanoce, S. Bertoni, J. et al., *FASEB J.* 2009, **23**, 442-450.
29 E. Krieger, G. Vriend, *Bioinformatics* 2014, **30**, 2981-2982.
30 E. Krieger, K. Joo, J. Lee, J. Lee, S. Raman, J. Thompson, M. Tyka, D. Baker, K. Karplus, *Proteins* 2009, **77** *Suppl 9*, 114-122.
31 A. Jakalian, D. B. Jack, C. I. Bayly, *J. Comput. Chem.* 2002, **23**, 1623-1641.
32 J. Wang, R. M. Wolf, J. W. Caldwell, P. A. Kollman, D. A. Case, *J. Comput. Chem.* 2004, **25**, 1157-1174.
33 S. Peherstorfer, H. H. Brewitz, A. A. Paul George, A. Wißbrock, J. M. Adam, L. Schmitt, D. Imhof, *Biochim. Biophys. Acta - General Subjects* 2018, **1862**, 1964-1972.
34 C. A. Bäuml, A. A. Paul George, T. Schmitz, P. Sommerfeld, M. Pietsch, L. Podsiadlowski, T. Steinmetzer, A. Biswas, D. Imhof, *Eur. J. Med. Chem.* 2020, 112474.
35 A. A. Paul George, P. Heimer, E. Leipold, T. Schmitz, D. Kaufmann, D. Tietze, S. H. Heinemann, D. Imhof, *Mar. Drugs* 2019, **17**, 390.
36 N. Schneider, G. Lange, S. Hindle, R. Klein, M. Rarey, *J. Comput. Aided Mol. Des.* 2013, **27**, 15-29.
37 T. Kühl, N. Sahoo, M. Nikolajski, B. Schlott, S. H. Heinemann, D. Imhof, *Chembiochem.* 2011, **12**, 2846-2855.
38 N. A. Kalogriopoulos, S. D. Rees, T. Ngo, N. J. Kopcho, A. V. Ilatovskiy, N. Sun, E. A. Komives, G. Chang, P. Ghosh, I. Kufareva, *Proc. Natl. Acad. Sci. U. S. A.* 2019, **116**, 16394-16403.
39 A. S. Konagurthu, J. C. Whisstock, P. J. Stuckey, A. M. Lesk, *Proteins* 2006, **64**, 559-574.
40 I. Reulecke, G. Lange, J. Albrecht, R. Klein, M. Rarey, *ChemMedChem* 2008, **3**, 885-897.
41 F. Madeira, Y. M. Park, J. Lee, N. Buso, T. Gur, N. Madhusoodanan, P. Basutkar, A. R. N. Tivey, S. C. Potter, R. D. Finn, et al., *Nucleic Acids Res.*2019, **47**, W636-W641.
42 C. A. Johnston, F. S. Willard, M. R. Jezyk, Z. Fredericks, E. T. Bodor, M. B. Jones, R. Blaesius, V. J. Watts, T. K. Harden, J. Sondeket al., *Structure* 2005, **13**, 1069-1080.
43 D. Frishman, P. Argos, *Proteins* 1995, **23**, 566-579.